Università degli Studi di Padova

Department of Information Engineering

Master's Degree in Bioengineering

Classification of EEG and fNIRS signals from Completely Locked-in State Patients for a Brain-Computer Interface communication system

Supervisor
Alessandra Bertoldo
Università degli Studi di Padova

Co-supervisor
Ujwal Chaudhary
Niels Birbaumer
Institute of Medical Psychology and Behavioural Neurobiology, Tübingen

Master Candidate
Giulia Corniani

3rd December 2018

ai miei genitori, Tiziana e Giorgio
e ai miei fratelli, Enrico e Francesco

Abstract

People suffering from complete motor paralysis with no severe deficiency in cognitive abilities, syndrome called Completely Locked in State (CLIS), remain aware of their surroundings without being able to interact and communicate in any way.

In this context, the only possibility of communicating with the social environment is by the techniques of Brain-Computer Interface.

Several efforts have already been made to develop BCI-based communication systems for CLIS patients; while any attempt to use EEG signals was unsuccessful, discreet and good results were obtained using the signals acquired with near-infrared spectroscopy techniques (fNIRS signals).

In this work, the focus is on the techniques of features extraction and selection on EEG and fNIRS signals and, finally, on the combination of the two to develop a system capable of classifying affirmative and negative answers from users in CLIS. The proposed analysis is entirely offline but has been carried out taking into account the constraints of a possible online system. The analysis considers the data collected in 4 visits to one patient. The choice to focus on a single case was made because the psychophysical considerations on the state of the patient are fundamental for a correct interpretation of the results and the author of this work had the opportunity to participate directly in the acquisition of some of these data.

Offline analysis led to good results in the classification of fNIRS signals, according to the different psychophysical states of the patient. Once again, using EEG signals it was not possible to successfully classify yes/no answers. Finally, the combination of the characteristics extracted from the EEG and fNIRS signals did not improve the performance of the system.

Preface

I worked on this thesis during a 5 months traineeship at the Institute of Medical Psychology and Behavioral Neurobiology of Tübingen where I joined the group lead by Ujwal Chaudhary and Niels Birbaumer.
During this period as intern student, I had the opportunity to actively contribute to design and improve communication BCI-based systems for LIS and CLIS patients affected by ALS.

I also participated in a one week visit to Patient6. There, I could practically test our work but, most of all, I could understand what it means relating to patients and their families.
I have experienced how emotional and psychological aspects are a fundamental part of our work and how gaining the confidence of the patient and his family is essential because collaboration is the only means to achieve good results.

Contents

List of figures

List of tables

List of acronyms

ALS	Amyotrophic Lateral Sclerosis
BCI	Brain-Computer Interface
CLIS	Completely Locked-in State
DPF	Differential Path-Length Factor
EEG	Electroencephalogram
EMG	Electromyogram
EOG	Electrooculogram
FIR	Finite Impulse Response
fNIRS	Functional Near-Infrared Spectroscopy
HbO	Oxyhemoglobin
HbR	Deoxyhemoglobin
HbT	Total Hemoglobin
LIS	Locked-in State
mRMR	Maximum-Relevance Minimum-Redundancy
NIR	Near-Infrared
PSD	Power Spectral Density
SVM	Support Vector Machines
tDCS	transcranial Direct Current Stimulation

1

Introduction

Communication is the manifestation of many verbal and non-verbal skills, like languages, gestures, facial expressions, body movements, voice tones, written texts, and it is the process of sharing thoughts, intentions, emotions, and feelings with other human beings.

Due to some disease, like Amyotrophic Lateral Sclerosis (ALS), patients progressively lose the control of any voluntary muscles and eventually are in a completely paralyzed state, known as Completely Locked-in State (CLIS), without severe deficiency in cognitive abilities. Since all the possible ways of communication are based on the use of some voluntary motor controls which activate and make body muscles move, subjects in CLIS are completely unable to communicate and interact with the social environment. The inability to communicate prevents patients from expressing their basic needs. The lack of communication, besides being a factor of psychological challenge for the patients themselves, greatly exacerbates the difficulties faced by the families and caregivers of people in CLIS.

In this scenario, the Brain-Computer Interface (BCI) techniques represent a good, and at

the moment the only one, chance to re-establish communication with CLIS patients.

This work presents a BCI system to recognize yes and no answers to questions presented to a CLIS subject. The "incipit" is an already existing BCI system (see Section 1.3), developed by Chaudhary et al. and presented in [1]. This is able to classify yes and no answers, with discreet performance, using exclusively the change in oxygenated hemoglobin signal. Here, the focus is on the techniques of features extraction and selection used before the classification phase, where a simple SVM classifier is adopted, trying to achieve a stable and performing system. To do this, different biological signals are recorded and analyzed, comparing their characteristics and suitability for differentiating yes and no answers.

In the following, first of all, a brief and general overview of BCI systems, the acquisition techniques used, the Locked-in Syndrome and the Amyotrophic Lateral Sclerosis is proposed to introduce in the specific topic. In the second chapter, the acquisition protocol and the signals analysis and classification methods are explained. Then, in chapter 3 and 4, the results are presented and discussed with some proposals for improvements and future works. Finally, in the conclusive chapter, there is an overview of the whole work.

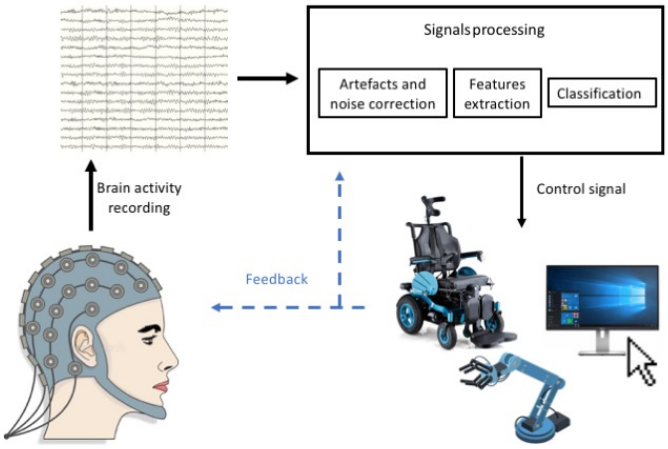

Figure 1.1: *General components of a BCI system:*
in each BCI system we can identify four main components: the user, the acquisition device, the translation block, and the actuation devices

1.1 Brain Computer Interface

A Brain-Computer interface system uses the neural activity generated by the brain to provide communication and control channels to its users, bypassing the brain's normal output channels of peripheral nerves and muscles. For this reason, BCI represents a useful augmentative technology for those who are unable to generate voluntary muscular movement due to severe motor disabilities.

The term "brain-computer interface" (BCI) was used for the first time in 1973 by the French neurophysiologist Jaques Vidal, who predicted the possibility of combining the incoming technological power of the computers and the possibility of recording the brain activity. In the same period, studies conducted by Joe Kamiya demonstrated that healthy persons could learn to voluntary change the alpha waves of their EEG signal, process known as "neurofeedback", which opened the way of the BCIs studies. [2]

The goal of a BCI system is to enable the user to control the external device by using his/her brain activity. Almost all the BCI systems have four main components:

1. *Users:* is any entity that can relay its intent by intentionally altering its brain state to

generate the control signals used as input for the BCI system.

2. *Acquisition devices:* BCI systems can use invasive or noninvasive techniques to record brain activity. Computerized tomography (CT), positron electron tomography (PET), magnetic resonance imaging (MRI), functional magnetic resonance imaging (fMRI), magnetoencephalography (MEG), functional near-infrared spectroscopy (fNIRS) and electroencephalography (EEG) have been used for noninvasive acquisitions. However, the most prevalent methods are EEG and, lately, fNIRS as both of them are relatively easy to use, cheap and portable devices, desirable features for such systems. The low spatial resolution and the distance of the electrode from the source of the signal, with consequent problems of noise and attenuation, are the main problems of these devices. These are the techniques used in this work and further explained in the following sections.

   The invasive technique requires a surgery to implant microelectrodes in the cortical area of the brain to record the activity even of few neurons. The main advantage is the quality of the signals acquired invasively: they aren't attenuated and the noise components are quite absent. On the other hand, in addition to the risks and disadvantages associated with surgery, this kind of electrodes has a limited lifetime and has a stable recording capability of some months.

3. *Translation block:* here, the brain signal is converted into a command signal. The acquired digitalized signals are, first of all, processed to maximize the signal-to-noise ratio (SNR) removing noise and artifacts (i.e. movements due to eyes blink, breath, heartbeat etc.). Then the features extraction process obtain the characteristics of the signals that can better reflect the users' intent. A classification algorithm is finally used to associate the features with one of the possible output commands of the system. Different approaches can be used in this phase according to the characteristics of the signal and the purpose of the system.

4. *Actuation device:* it is composed of physical (i.e. robotic arm, wheelchair, ecc.) and software components (i.e. communication systems for world spelling, yes/no answers etc.). The device receives control signals from the translation block and uses them to

drive an application. The functioning of the device gives the feedback to the user and a feedback signal is also sent to the processing block to update the state of the system.

Each BCI system has some distinctive characteristics. These include the input signals; the translation algorithm; response time, speed and accuracy and their combination into information transfer rate; type and extent of user training required, appropriate user population; appropriate applications; and constraints imposed on concurrent conventional sensory input and motor output (e.g., the need for a stereotyped visual input, or the requirement that the user remain motionless). [3]

Since the effectiveness of BCI depends on the capability of the user to control his/her brain activity, training methods are necessary to learn how to control the system. The main approaches for the training are cognitive task, when the user is asked to perform voluntary and conscious mental activity, like image to move a limb, or operant conditioning, where the users think about anything and the feedback provided by the system serves to condition the user to continue to produce and control the components that have achieved the desired outcome. Multiple factors, like concentration, distraction, frustration, emotional state, fatigue, motivation, and intentions can affect the results. For this reason, the feedback loops play a fundamental role in the good performance of all the BCI systems, informing each component of the state of the devices and representing a reward for the user's attempts.

1.1.1 Electroencephalography

The electroencephalogram (EEG) is the measure of the electrical activity of the brain recorded from electrodes placed on the scalp. The first EEG recording was made by the German psychiatrist Hans Berger in 1924. The EEG devices record the potential differences between electrodes which reflects the current density that arises from the action of a chemical transmitter on postsynaptic cortical neurons. The action causes localized depolarization, that is an excitatory postsynaptic potential (EPSP), or hyperpolarization, that is an inhibitory postsynaptic potential (IPSP).

The potential differences are measured either between pairs of scalp electrodes (bipolar) or between individual electrodes and a common reference point (unipolar). In the second arrangement, the reference point is usually a relatively inactive site on the scalp.

The amplitude of the EEG signals for healthy subjects is about 100 μV while the bandwidth is from under 1 Hz to about 50 Hz. From the EEG signal, it is possible to differentiate alpha (α), beta (β), delta (δ), theta (Θ) and gamma (γ) waves, according to different frequency spectrum. In Table 1.1 the typical frequency bands, their characteristics, and locations are reported.

The placement of the electrode on the scalp is generally based on the international 10-20 system, in which the measurements from four standard position on the head (nasion, inion, right and left preauricular points) determine the position of 21 electrodes. High density electrode settings use up to 320 electrodes and the 10-10 (see Figure 1.2) or 10-5 placement systems.

In the clinical contest, EEG recordings are used to investigate the brain's spontaneous electrical activity over a period of time, the event-related potentials, the spectral content of the signals and to diagnose epilepsy, sleep disorders, depth of anesthesia, strokes, coma, encephalopathies, and brain death.

EEG recordings have a high temporal resolution since the devices have a sampling rate ranging between 250 and 2000 Hz. The spatial resolution of this technique is low and the exact areas of activations can be identified only with sophisticated methods of spatial filtering and interpolation.

	Frequency Band	Characteristic stage	Location
Delta	0.5-4 Hz	Deep sleep	Deep structures
Theta	4-8 Hz	Relaxation, drowsiness, sleep	Frontal regions
Alpha	8-14 Hz	Relaxation, thinking, closed-eyes	Occipital regions
Beta	14-30 Hz	Active thinking, focus, high alert,	Parietal and frontal lobes
Gamma	>30 Hz	Combination of sensory processing	Somatosensory cortex

Table 1.1: *EEG characteristic waves:*
In the EEG signals, it is possible to differentiate five different waves according to different frequency bands

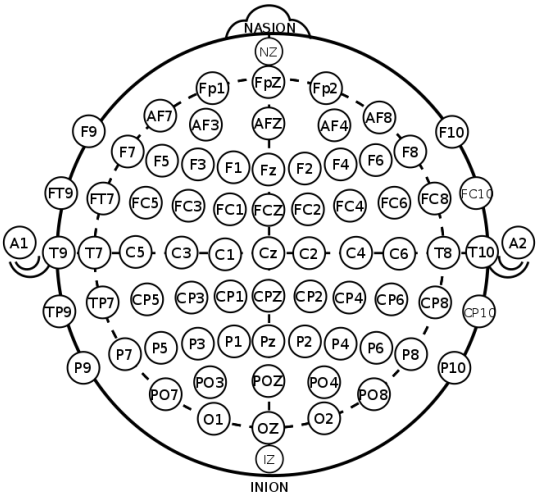

Figure 1.2: *10-10 system for electrodes placement*

EEG signals can be affected by many kinds of biological, instrumental or environmental noise and artifacts. Bioelectric artifacts can be generated by any kind of movement, (eye and chew movement particularly affect EEG recordings due to the closeness with the scalp), heartbeat, sweat, and breath. In general, artifacts are recognized because of their temporal relationship to other bioelectrical signals, like electrocardiogram(ECG), electrooculogram (EOG) or electromyogram (EMG), because of their unusual appearance, or because the electrical field of the event is hard to interpret in a biologically plausible manner. [4]

Furthermore, scalp EEG electrodes are mostly sensitive to activity correlated over large areas of the superficial cortical area of the brain, with smaller contributions from deeper sources.

The acquisition of the brain activity based on the same principles of EEG using microelectrodes implanted in the brain is named Electrocorticography (ECoG), or intracranial electroencephalography (iEEG). These techniques allow the measurement of the bioelectric events produced by single neurons with invasive micro-electrodes targeting the cells of interest. The amplitude of the signals measure directly on the surface of the brain with invasive microelectrodes is about 1-2 mV.

1.1.2 Functional Near-Infrared Spectroscopy

Near-infrared spectroscopy (NIRS) is a neuroimaging technique which uses light in the near infrared range (650nm- 900nm) to study the functional activity of the brain. The possibility of evaluating the absorption and scattering proprieties of the near-infrared light (NIR) to study the brain activation was for the first time discovered in 1977 by Jobsis [5]

During NIRS, the source optodes placed on the head surface emit a NIR light beam. An attenuated and scattered signal, after traveling through the cortical regions of the brain, is received by some detector optodes placed on the scalp at a certain distance from the source optode. The acquired signals are processed to quantify the cerebral oxygenation and changes in oxy (HbO), de-oxy (HbR) and total hemoglobin (HbT). [6]

The neuronal activation in response to a stimulus involves secretion of neurotransmitters, change in the size of surrounding cells, vasodilation or constriction, change in the cerebral blood flow and change in oxygenation state of the blood in the brain. [7] [8] NIRS measures these responses of the cerebral blood vessels, i.e. the change in cerebral blood flow and the change in oxygenation state of blood in the brain, to evaluate the brain activation and functionality.

In the human brain, there are different light absorbing species named chromophores, such as water, cytochrome c oxidase, and hemoglobin. The brain is opaque to the visible range of light, as this is strongly absorbed by water and cerebral tissues. Conversely, in NIR range, light absorption by water and tissues changes drastically, and the only dominant chromophores present at this wavelength are cytochrome c oxidase and hemoglobin. The content of hemoglobin within the brain tissue is approximately 600mg/100mg tissue, which is several times the concentration of cytochrome oxidase. Thus, the dominant chromophore present in the brain during NIRS acquisitions is hemoglobin, which accounts for the majority of light attenuation and scattering in the brain. [9]. Since the scattering event of photon dominates the absorption event, the optical transport of light in the brain is scattering dominant. Thus, light in the range of 650-900nm is minimally absorbed and preferentially scattered by

the hemoglobin present in the brain. [10] [11] In particular, NIR light of wavelength close to 690 nm and 830 nm provide dominant information about HbR and HbO, respectively. [12]

The light transport model used to describe the attenuation of light as it passes through the highly scattering brain media is the Modified Beer-Lambert Law. The Beer-Lambert law quantifies the attenuation of light at given a wavelength when it passes through a media containing chromophores using the Equation 1.1:

$$A(t,\lambda) = log(\frac{I(t,\lambda)}{I_0(t,\lambda)}) = \varepsilon(\lambda) * C(\lambda) * d(\lambda) \tag{1.1}$$

where: $A(t,\lambda)$ is the attenuation of the λ wavelength light crossing the given media at time t; $I(t,\lambda)$ is the intensity of the λ wavelength light transmitted out of the given media at time t; $I_0(t,\lambda)$ is the initial intensity of the λ wavelength light incident on the media at time t; $\varepsilon(\lambda)$ is the molar extinction coefficient of a chromophore at λ of wavelength light, expressed in $mM^{-1}cm^{-1}$; $C(\lambda)$ is the concentration of chromophore in the media at λ of wavelength light and $d(\lambda)$ is the direct path length of a photon from the emitting to the receiving optode placed on the media surface, at λ of wavelength light.

The Beer-Lambert law is true only for purely absorbing media. For scattering media such as the brain, the modified Beer-Lambert law has to be used, which takes into account the attenuation due to scattering in the media and the changes in the path length of the photon due to its scattering. Indeed, in highly scattering media the path length of the photon is greater than the geometrical distance between the optodes because of the scattering events. Delpy et al. [13] defined a scaling factor to correct for the path-length: the differential path-length factor (DPF). Thus the modified Beer-Lambert law is described by the expression shown in Eq. 1.2

$$A(t,\lambda) = log(\frac{I(t,\lambda)}{I_0(t,\lambda)}) = \varepsilon(\lambda) * C(\lambda) * d(\lambda) * DPF(\lambda) + G(\lambda) \tag{1.2}$$

where *DFP(λ)*is the differential pathlength factor at λ of wavelength light as defined by Delpy [13], and it depends on the number of scattering events that occur. *G(λ)* is an unknown term representing scattering coefficient of the tissue together with the geometry of the optodes. Therefore, an absolute calculation of chromophore concentration cannot be derived from Eq. 1.2. However, it is possible to calculate changes in the concentration of chromophores by calculating changes in optical density (i.e. A(t, λ)) at two different wavelengths of light in order to cancel out the *G* term, assuming the same value of *G(λ)*for all chromophores in the medium: [14]

$$\Delta OD\lambda_1 = \varepsilon^{\lambda_1}_{HbR} * L * [HbR] + \varepsilon^{\lambda_1}_{HbO} * L * [HbO] \tag{1.3}$$

$$\Delta OD\lambda_2 = \varepsilon^{\lambda_2}_{HbR} * L * [HbR] + \varepsilon^{\lambda_2}_{HbO} * L * [HbO] \tag{1.4}$$

In Eq. 1.3 and 1.4, $\Delta OD\lambda_1$ and $\Delta OD\lambda_2$ are the changes in optical density at λ_1 and λ_2 respectively, while $\varepsilon_{HbO}{}^{\lambda_1}$, $\varepsilon_{HbO}{}^{\lambda_2}$, $\varepsilon_{HbR}{}^{\lambda_1}$ and $\varepsilon_{HbR}{}^{\lambda_2}$ are the absorption coefficient of HbO and HbR at λ_1 and λ_2. L is the effective average pathlength of light through the tissue. L is obtained from the product of the actual source-detector separation and DPF. The source-detector separation is measurable along the surface of the head, and the extinction coefficient for a given chromophore can be looked up in tables [15].

Using the Eq.1.3 and 1.4 the change in otpical density is calculated and used to evaluate the changes in concentration of Hbo and HbR: Δ[HbO] and Δ[HbR]. The wavelength chosen in this case are λ_1=*830 nm* and λ_2=*690 nm* as the most sensitive to the changes in, respectively, HbO and HbR concentrations. Knowing Δ[HbO] and Δ[HbR] is also possible to evaluate the change in the total hemoglobin as:

$$\Delta[HbT] = \Delta[HbO] + \Delta[HbR] \tag{1.5}$$

NIRS technologies can be used to obtain either spectroscopy signals or, if the number of optodes is sufficiently big, the signals are reconstructed to obtain an image called Diffuse Op-

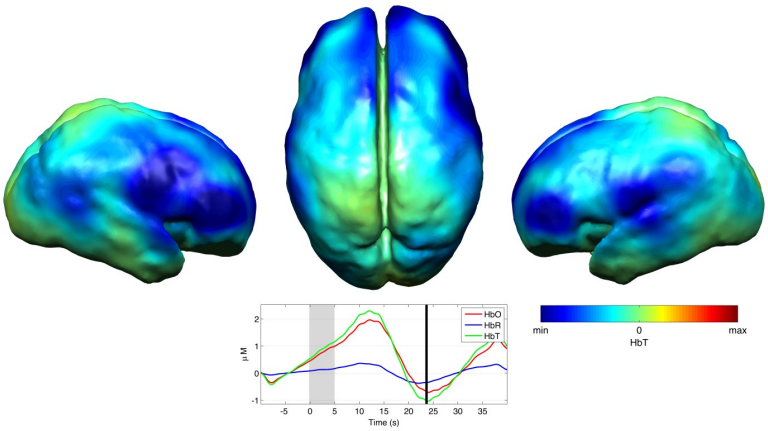

Figure 1.3: *Diffuse Optical Image obtained with NIRS*
When a high number of optodes is used to record the change in HbO, HbR, and HbT, it is possible to reconstruct images to map the behavior of different brain regions.

tical Imaging (DOI) representing the cerebral oxygenation and hemodynamics. (see Figure 1.3) [16]

NIRS provides excellent temporal resolution and a reasonable spatial sensitivity. Additionally, NIRS is robust to movement artifacts, enabling investigations during routine human activity in moving subjects. [15] With this characteristic, NIRS could override the most used neuroimaging techniques for hemodynamic studies, the functional magnetic resonance, which has low temporal resolution and is highly susceptible to movement artifacts.

The major limitation of NIRS is reduced depth penetration of NIR light in the brain, which limits its capability to investigate hemodynamics only to the surface of the cerebral cortex. [16]

1.2 Locked-in and Completely Locked-in State

Locked-in syndrome was defined for the first time in 1966 by Plum and Posner as quadriplegia, anarthria, and paralysis of all the facial muscles, except the vertical eye movement, due to bilateral lesions of the corticospinal and corticobulbar tracts in the ventral portion of the pons. [17]

The cause of the Locked-in syndrome can be ischemic, hemorrhage, traumatic, tumor, metabolic, infectious, systemic: neurological disease such as ALS, end-stage Parkinson, multiple sclerosis can lead to a Locked-in State (LIS) with different etiological and neuropathological features. [18] [19].

Patient affected by the Locked-In syndrome are completely conscious but, attention, intellectual ability, perception, visual and verbal memory can sometimes be affected. [20] Hearing is usually well preserved, while, visual difficulties can arise from blurring and diplopia. [18] Due to the many different possible causes, this syndrome is not a homogeneous neurological entity but has numerous variations. Locked-in syndrome can be differentiated into three categories:[21]

- *Classic:* total paralysis, except for eyes movements and blinking, and preserved consciousness (LIS)
- *Incomplete:* total paralysis, with remnants voluntary movement other than eye movement, and preserved consciousness
- *Complete:* total paralysis and inability to communicate and preserved consciousness. (Completely locked-in State, CLIS)

The capability to move the eyes enable people in LIS to use non-verbal communication devices, like eyes tracker, or to adopt many strategies to answer simple close questions. This is also a fundamental tool to confirm the diagnosis and assess consciousness and cognitive capabilities.

The cerebral metabolism can distinguish subjects in LIS/CLIS from patients in vegetative state; indeed, as reported by Zeman in studies with positron emission tomography [22], the cerebral metabolism is middle reduced in LIS/CLIS subjects, while severely reduced in the others. Furthermore, the EEG-reactivity (event-related synchronization (ERS), and event-related desynchronization, (ERD)) can differentiate LIS/CLIS from Coma. [23]

Pulmonary complications are the leading cause of death for LIS patients: dysphagia and impaired cough reflex leads to further complications, including atelectasis and pneumonia; immobility predisposes to pulmonary embolus.[18]

1.2.1 Amyotrophic lateral sclerosis

Amyotrophic lateral sclerosis is a neurodegenerative disease characterized by the progressive degeneration of motor neurons in the primary motor cortex, corticospinal tracts, brainstem and spinal cord which leads to a progressive paralysis of the voluntary muscles. The term "amyotrophic" refers to the muscle atrophy, weakness, and fasciculation, while "lateral sclerosis" refers to hardening of the anterior and lateral corticospinal tracts as motor neurons in these areas degenerate and are replaced by gliosis.[24] The exact cause of motor neuron degeneration in ALS is unknown but is likely to be a complex interplay between multiple pathogenic cellular mechanisms, including genetic factors (mutations in the Copper-Zinc superoxide dismutase (SOD1) gene cause a toxic gain of function), excitotoxicity (a neuronal injury induced by excessive glutamate. An overstimulation of glutamate receptors results in massive calcium influx into the neurons, leading to increased nitric oxide formation and, finally, neuronal death), oxidative stress (accumulation of reactive oxygen species (ROS) causes cell death and consequently neurodegeneration), mitochondrial dysfunction, impaired axonal transport, neurofilament aggregation, protein aggregation, and inflammatory dysfunction. [24] [25]

ALS is relentlessly progressive; 50% of patients die within 30 months of symptom onset and about 20% of patients survive between 5 years and 10 years after symptom onset. Respiratory failure and complications are the usual cause of death in ALS.

A crucial moment in the progress of the disease occurs when the patient is no longer able to breathe and feed autonomously. At this point, those who decide to stay alive are subjected to artificial ventilation and PEG (Percutaneous Endoscopic Gastrostomy) nutrition, developing a profound motor paralysis state recognized as Locked-in syndrome, with incomplete

and, eventually, complete classification. The time elapsing between the onset of the disease, the need for ventilation and artificial nutrition, been in LIS and CLIS has a great variability between subjects.

As reported by Kiernan [26], the incidence of ALS in Europe is uniform at 2,16 per 100000 person-year while a worldwide estimation of the disease is not available. Men have a higher incidence (3 per 100000 person-year) than women (2,4 per 100000 person-year) and the lifetime risk of ALS is 1:400 for woman and 1:350 for men.

The diagnosis of ALS is mainly based on the presence of very characteristics clinical findings but, since there is no specific diagnostic test, it is sometimes difficult to distinguish between ALS and other motor neuron diseases. The 'El Escorial' diagnostic criteria [27], developed by the World Federation of Neurology (WFN) Research Group on Motor Neuron Diseases, and the revised 'Airlie House' criteria [28] defines some clinical, electrophysiological and neuroimaging features to establish the level of diagnostic certainty. Degeneration signs of the Upper Motor Neuron (UMN) and Lower Motor Neuron (LMN) are the main features representing ALS and they can be examined in four regions (bulbar, cervical, thoracic and lumbosacral) considering clinical, electrophysiological or neuropathologic examinations and evaluating the progressive spread of signs within a region or to other regions. The signs of degeneration for the LMN are weakness, wasting and fasciculation, while, for the UMN, pathologically increased reflexes and spasticity; these can be found by physical and neurological examination. Neuroimaging techniques, in particular, MRI, mainly contribute to excluding alternative pathological causes, as much as electrophysiological investigations, like nerve conduction studies and electromyography. There are no clinical laboratory tests which confirm the diagnosis of ALS.

1.3 State of the art: communication and BCIs for CLIS patients

The first BCI for communication in ALS patients with intact eye muscles (LIS) was presented by Birbaumer et al. in 1999[29]; since then, several successful invasive and noninvasive BCI

systems have been developed for communication in LIS patients affected by ALS or other diseases, with the possibility for the subject to spell words and compose sentences. Though, none of the BCI techniques used with LIS patients are able to provide the same means of communication for the patients in CLIS due to ALS. All the existing BCIs for communication, indeed, rely on two elements: first, the neuro-electric signal (EEG or ECoG) control and second at least an intact eye muscle; thus, so far, all the systems designed for LIS subjects did not work in patients in CLIS, in which eye movement control is lost.

Chaudhary et al [1] developed fNIRS based BCI system for communication in CLIS patients.

In this study, which was the first of its kind, fNIRS-based BCI was used for binary communication in four ALS patients in CLIS. Several questions with known yes or no answer were presented to the subjects while fNIRS, EEG from fronto-central brain regions and EOG signals were acquired. After training a classifier separating "yes" from "no" answers for several days, the patients were given feedback of their response to questions with known answers and open questions. In each session, fNIRS, EEG and EOG signals were recorded but the online analysis and the feedback were provided only using the HbO signal from fNIRS. Chaudhary et al. [1] reported that four patients in CLIS communicated with frontocentral cortical oxygenation-based BCI with an above-chance-level correct response rate over 70% during a period of several weeks.

The change in HbO, EOG, and EEG signals in response to true and false questions, obtained from the frontocentral region of the brain, were used in the offline analysis to determine the SVM classification accuracy of yes and no answers. The analysis performed using the EEG signals in the time domain across all the training sessions showed no significant differences between yes and no thinking, as well as the analysis of eye movements measured with EOG. The EEG signal was also studied to evaluate the correlation between fNIRS classification accuracy and low-frequency bands mean power since these bands are the most related with vigilance. In three out of four patients, a negative averaged correlation was found be-

tween low-theta band mean power and fNIRS classification accuracy.

2

Material and method

2.1 Patient and visits

The following analyses consider the data acquired from a single patient, hereinafter referred to as Patient 6.

Patient 6 (Male, 38 years old, CLIS) was diagnosed with bulbar ALS in 2009. He lost speech and capability to move by 2010. He has been artificially ventilated since September 2010 and is in home care. No communication with eye movements, other muscles, or assistive communication devices was possible since 2012.

Patient 6 was visited in total 7 times from May 2017 to September 2018. In three of the visits (v02, v03, and v04) different studies were performed (stimulation, evoked potential, motor imagery etc.) and none of the BCI acquisition followed the ”standard” protocol (see section 2.3). The details of each visit are reported in Table 2.1

Visit Name	Date	BCI sessions	Acquisition channels
v01	29-05/02-06-2017	6	FC5, FC6, C5, C6, Cz, EMGUL, EMGDL, EMGUR, EMGDR,EOGUL, EOGDL, EOGUR, EOGD 8 fNIRS source optodes + 8 fNIRS detector optodes
v02	11-09/16-09-2017	0	//
v03	28-09/02-10-2017	0	//
v04	02-11/06-11-2017	0	//
* v05	14-04/17-04-2018	4	R1, R2, L1, L2, Cz, C1, C2, EOGU,EOGD,EOGL, EOGR 8 fNIRS source optodes + 8 fNIRS detector optodes
v06	21-05/25-05-2018	5	R1, R2, L1, L2, Cz, C1, C2, EOGU, EOGL, EOGR 8 fNIRS source optodes + 8 fNIRS detector optodes
v07	24-09/29-09-2018	4	R1, R2, L1, L2, C1, C2, Cz, Fz, P3, P4, Pz, EMGL, EMGR, EOGR, EOGU, EOGL 8 fNIRS source optodes + 8 fNIRS detector optodes

Table 2.1: *Details of the visits to Patient 6*

2.2 Instrumentation

2.2.1 EEG acquisition

During the BCI sessions, the EEG, EOG and EMG signals were recorded with a multi-channel EEG amplifier (V Amp DC, Brain Products, Germany) using different number and position of Ag/AgCl active electrodes.

The table 2.1 shows the positions of the electrodes, in each visit, according to the international system 10 - 10 (see Figure 1.2), except for the electrodes L1, L2, R1 and R2 which were

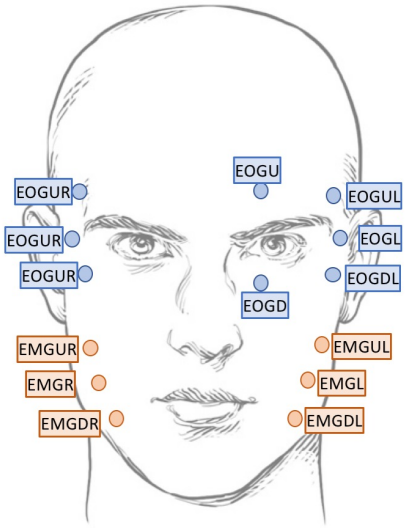

Figure 2.1: *Placement of EOG and EMG electrodes*

not positioned in the standard position but slightly shifted from the positions F4 (R1), FC4 (R2), F3(L1) and FC3 (L2) to allow the insertion of the optodes for the acquisition of the fNIRS signals. The placement of EOG and EMG electrodes is shown in Figure 2.1.

Each channel was referenced to an electrode on the right mastoid and grounded to the electrode placed at Fpz location of the scalp. Electrode impedances were kept below 10 kΩ and the EEG signal was sampled at 500 Hz.

2.2.2 fNIRS acquisition

A continuous wave (CW)-based fNIRS system, NIRSPORT (NIRx Medical Technologies [30]) was used. This performs dual-wavelength (760 nm and 850 nm) CW near-infrared spectroscopic measurement at a sampling rate of 7,81 Hz.

The NIRS optodes were placed on the frontocentral brain regions. In all the visit, 8 source optodes and 8 detector optodes were used, placed as shown in Figure 2.2.

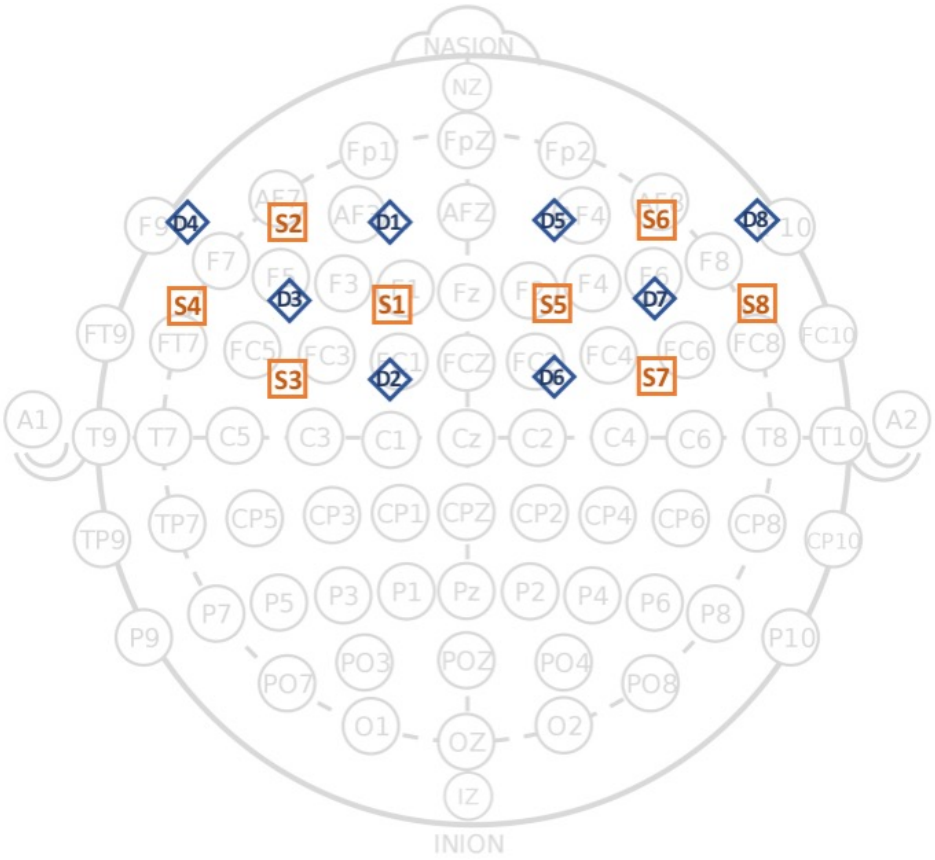

Figure 2.2: *fNIRS optodes placement:*
arrangement of the optodes in the front-central region of the head with reference to the position of the EEG electrodes in the international 10-10 system. The optodes represented in orange are the NIR light sources while those in blue are the detectors.

2.2.3 Software

The EEG signals were imported and stored using Brain Vision Analyzer provided by Brain Products GmbH. [31]

The fNIRS signals were imported and stored using NIRStar provided by NIRx Medical Technologies. [30]

All the analysis were done using the software Matlab_2018a.

2.3 Acquisition Protocol

In the following sections, a block is a single continuous signals acquisition while a session is considered as a set of subsequent acquisition blocks, even of different kinds and with different tasks performed by the patient. Before every single block, the patient is clearly instructed to the task he's required to perform during the following acquisition.

For the purposes of this work, which consists of the offline study of a classification method, only the blocks of training and feedback will be equivalently considered and analyzed.

Throughout all the acquisition period, the EEG signal was continuously visually monitored to avoid long periods of slow-wave sleep during the BCI evaluation.

2.3.1 Preliminary recordings

Every session started with 10 minutes of resting state EEG and fNIRS signals recording. In this phase, the patient was instructed to relax and to not think. Secondly, transcranial Direct-Current Stimulation (tDCS) was performed for 10 minutes. During the tDCS, EEG and fNIRS signals were also acquired. Finally, 10 more minutes of resting state EEG and fNIRS signals were recorded.

Transcranial Direct-Current Stimulation (tDCS) is a non-invasive stimulation technique that delivers a low electric current to the scalp. A fixed current between 1 and 2 mA is typically applied. tDCS works by applying a positive (anodal) or negative (cathodal) current via electrodes to an area, facilitating the depolarization or hyperpolarization of neurons, respectively. Naro et al. in [32], demonstrated that a-tDCS was able to boost cortical connectivity and excitability in healthy subjects as well as in patients with Disorders of Consciousness (DOC) and thus could improve the patient responsiveness and attention during the following BCI acquisitions.

The main purpose of the resting state acquisition before and after the tDCS is to control the effectiveness of the stimulation but this kind of analysis is beyond the scope of this work.

Event	Trigger value		
	Yes Question	No Question	Open Question
Acquisition Start	9		
Baseline	10	11	12
Question Presentation	5	6	7
Thinking Period	4	8	13
Feedback	1	2	3
Acquisition end	15		

Table 2.2: *Triggers values:*
Values of the triggers used to record the onset of each event

2.3.2 Training blocks

The training blocks are the first part of the actual BCI protocol. In each block, 20 questions are presented to the patient: 10 with "yes" answer and 10 with "no" answer.

In this phase, the proposed questions must have a sure answer, like for example "Rome is the capital of Italy" or "Rome is the capital of Germany". ". Question formulation is crucial for the performance of the BCI system as it is very important to keep the patient motivated and avoid boredom. Hence all the questions are formulated with the help of the family based on the biography of the patient.

During a training block, EEG and fNIRS are acquired constantly. Using a triggering system, the onset of each event (acquisition start, baseline, question presentation, thinking period, feedback, acquisition end) is recorded in a vector. The triggers differentiate the events and the yes or no questions, as reported in Table 2.2 and displayed in Figure 2.3.

Before the presentation of a question, 5 seconds of baseline signals are acquired to check, if there is, the different brain activations during the questions listening and the response. The questions are recorded and presented through a speaker controlled by the BCI system to synchronize the timing. After the presentation of each question, 10 seconds of "thinking period" are acquired in which the subject is supposed to answer. The patient is informed by the system of the end of the thinking period through a vocal signal, usually a "thank you".

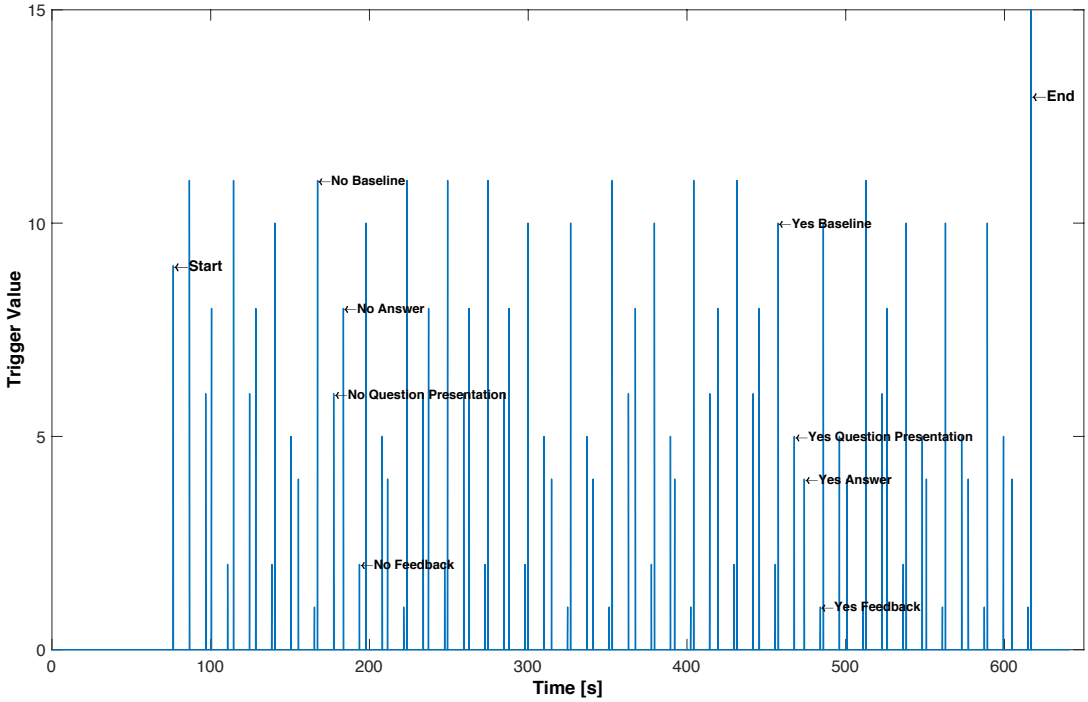

Figure 2.3: *Plot of a triggers vector*
Visual representation of a triggers vector used to record the onset of each event during the acquisitions. In particular, the vector plotted is from a training block of visit7 (v07_d1_b04)

The patient can be instructed differently on how to answer the questions. The most used method is to ask the patient to just keep thinking yes or no. Sometimes it's also possible to tell the patient to perform a task to answer yes and to do nothing to answer no. The task can be motor imagery or the attempt to move a muscle if there is the chance of some remain muscle control. The instructions should remain the same during a session to avoid confusing the patient and otherwise, it would be difficult, and even wrong, trying to find a model to describe and classify the signals afterward.

2.3.3 Feedback blocks

After at least two blocks of training in the same session, a model to predict the subject answers is built. Using the same closed questions of the training and instructing the patients exactly as before, after each thinking period, the signals are analyzed and classified by the model and

a feedback is given to the subject.

The feedback, in this case, consists of a voice informing how the signals corresponding to the last response were classified. This is very important to keep the patient focused, to gain his confidence in the BCI system and motivate him to continue answering questions that may seem trivial. Sometimes, to avoid the dejection produced by wrong feedbacks, it's possible to set the system so that only when the signals are correctly classified the complete feedback is reported to the patient and otherwise only a "thank you" informs on the end of the thinking period.

The acquisition procedure is the same used for the training blocks, with questions chosen from the same set, the same triggering system, and both EEG and fNIRS simultaneously acquired.

2.3.4 Open question blocks

The possibility to answer to open questions is, obviously, the final goal of this BCI system. To reach this stage, it is essential that the model, built and tested in the previous phases of training and feedback, gave excellent performance in terms of classification and stability.

The procedure is the same used for the previous blocks, with the recorded questions, the trigger system and the same time intervals for thinking and baseline periods. Only the number of questions in each block can vary.

Usually, to double check the accuracy of the classification, the same question is asked both in a positive and negative way, for example, that both "are you tired?" and "are you rested?" are asked. Furthermore, if the questions are particularly sensitive, they are asked many times and in different sessions.

When the system is stable, with an accuracy of response classification of more than 90%, the patient can use spellers to freely form words and phrases. To date, the use of such systems has only been possible with LIS patients.

2.4 Signals Processing

Given the different nature of EEG and fNIRS signals, they require different processing techniques to remove artifacts and all components not related to brain activity. The two different procedures applied are explained in detail in the next sections 2.4.1 and 2.4.2

2.4.1 Processing of EEG signals

For each performed block, a continuous EEG signal, of 10-12 minutes (about 300000-360000 samples) is recorded covering 20 questions asked to the subject and their response. The signals acquired by the amplifier are saved in .vhdr format and imported into the Matlab software using the "eeglab" tool.

First of all, the signals are brought back to null mean, i.e. the new signal $\bar{x} = [\bar{x_1}, \bar{x_2}, ..., \bar{x_N}]$ is obtained with:

$$\bar{x_i} = x_i - \frac{1}{N}\sum_{k=1}^{N} x_k \tag{2.1}$$

$$\text{for } i = [1 : N]$$

This operation is done to make possible the comparison of the characteristics of different signals and is done to the signals of all the channels.

The signals are then divided according to the triggers recorded extracting the 20 segments corresponding to the 10 seconds thinking periods, i.e the periods in which the patient was supposed to answer the questions.

The segmented signals corresponding to the EEG, EOG and EMG channels are then filtered separately to better preserve the characteristics of each type of signal.

To avoid signal distortions that could typically appear in the firsts and lasts samples of the signal after the filtering phase, every signal is cut 200 samples before the trigger representing the onset of the thinking period and 200 samples after the trigger representing the end of the thinking period. After the filtering, these 400 samples are removed.

The EMG signals are filtered using a bandpass finite impulse response (FIR) filter of fixed order n=400. According to the physiological characteristic of these signals, the bandpass is set at [2-70] Hz. The filter is designed using the function `fir1` provided by Matlab; a Gaussian window was used.

The EOG signals are filtered using the same kind of filter used for the EMG signals but the bandpass is set at [2-50] Hz.

Both the EOG and EMG signals are further filtered using a Notch filter with the notch located at 50Hz to avoid electrical noise. The filter, designed using the Matlab function `iirnotch`, is a second-order infinite impulse response (IIR) notch filter.

The choice of the filter order is made by mediating between the need for a not too high order that would otherwise, in online applications, dilate processing times, and a frequency response as close as possible to the required characteristics. For the offline analysis, in fact, we try to reproduce faithfully the processing operations used online to avoid large differences in final performance. For the same reason, a FIR filter is chosen.

The EEG signals are filtered in 5 different ways obtaining 5 different signals, to better capture all the characteristics and dynamics. In any case, the filter used is a bandpass FIR filter of n=400 order designed using the Matlab function `fir1`, with a Gaussian window; the only difference between the five filters is the bandpass.

The bands are chosen according to the characteristic waves of EEG signals reported in Table 1.1. In particular, the bandpass of the filters are set at [2-30] Hz obtaining the "wideband" signal, [0.5-4] Hz for the Delta-band signal, [4-7] Hz for the Theta-band signal, [7-15] Hz for the Alpha-band signal and [15-30] Hz for the Beta-band signal.

Higher frequencies are discarded because observing the spectrum of the signal before the filtering, it's impossible to recognized activity above the 30 Hz imputable as brain activation. It is known that in patients with ALS, the spectrogram of brain electrical activity is shifted to low frequencies compared to that of a healthy individual.

2.4.2 Processing of fNIRS signals

The raw optical data acquired at 830 nm and 690 nm is filtered using a bandpass filter (0.001-0.5 Hz) to remove the signals arising from systemic physiology. The optical signals acquired from the surface of the head is contaminated by systemic signals like the heartbeat, respiratory signal, and others. The filtered optical data is further normalized to remove the instrument effect.

The optical signals are then processed using modified Beer-Lambert law (see Section 1.1.2, Equations 1.2, 1.3, 1.4) to calculate the relative change in concentration of HbO and HbR.

For the acquisition of fNIRS signals, 8 optode sources and 8 optode NIR light detectors are used. The light emitted by one source is received by all the detectors and potentially 64 signals can be reconstructed. This makes no sense because very little intensity of the light emitted by a source is received by the farthest detectors. Sources and detectors are therefore coupled so that only the closest to each other form an acquisition channel. 20 acquisition channels are considered in the analysis, 10 on each side of each hemisphere as reported in Table 2.3

In the offline analysis, the fNIRS signals are first processed and then segmented according to the same triggering system used for EEG signals and shown in Table 2.2 and Figure 2.3.

2.5 Features Extraction

At this stage, some features are extracted from the time series recorded during the response periods.

A feature is an individual measurable property of the process being observed. The aim is to describe and quantify the signals trend in the time domain and, only for EEG signals, in the frequency domain. The final goal is to differentiate a yes and no thinking period.

Since we do not know in advance which features or set of features can best distinguish between a yes and a no and the variability of the signal implies that the features used to classify

Left hemisphere			Right hemisphere		
Source	Detector	Channel Name	Source	Detector	Channel Name
S1	D1	Ch. 1	S5	D5	Ch. 11
S1	D2	Ch. 2	S5	D6	Ch. 12
S1	D3	Ch.3	S5	D7	Ch. 13
S2	D1	Ch. 4	S6	D5	Ch. 14
S2	D3	Ch. 5	S6	S7	Ch. 15
S2	D4	Ch. 6	S6	D8	Ch. 16
S3	D2	Ch. 7	S7	D6	Ch. 17
S3	D3	Ch. 8	S7	D7	Ch. 18
S4	D3	Ch. 9	S8	D7	Ch. 19
S4	D4	Ch. 10	S8	D8	Ch. 20

Table 2.3: *Coupling of fNIRS optodes for signal reconstruction:*
Sources and detectors are named and placed as shown in Figure 2.2

can vary in different sessions, a large number of features are extracted in order to describe the signal in every aspect.

2.5.1 EEG features

All the features are extracted from the signals of each channel and of each frequency bands used to filter the signals (see Section 2.4.1). In the following, x is the vector, containing the N samples of the signal recorded during one thinking period, from one channel and filtered in one frequency band.

For the EEG signals, 29 different features are extracted and they can be divided into three categories: amplitude features, range features, and spectral features. The EEG features extracted for a single thinking period signal are $29 features * 5 bands * n_{channels}$

Many of the EEG features are taken and adapted from the software for Matlab 'NEURAL', developed by Toole [33].

Amplitude Features

The amplitude features consider the dynamic of the signals in the time domain. Each feature is calculated on every segment of the recorded signals representing the thinking period, x, which has approximately a length of $L = 5000 samples$

- *Total Power:* is the power of the signal in the time domain. It is evaluated as:

$$TotalPower = \frac{1}{N}\sum_{k=1}^{N} x_k^2 \tag{2.2}$$

- *Standard Deviation:* measure of variability of the signal about a mean value. It is estimated using the Matlab function `nanstd(x)`, which evaluate the standard deviation of the signal in x after removing all NaN values.

- *Skewness:* measure of the degree of asymmetry of the distribution of the data around the mean value. A symmetrical distribution of the data has skewness equal to 0, while, a negative skew commonly indicates that the tail of the distribution of the data is on the left side, and a positive skew indicates that the tail is on the right. It is calculated using the Matlab function `skewness(x)`.

- *Kurtosis:* it is an index of the Gaussianity of the data distribution. The kurtosis of any univariate normal distribution is 3; if >3 the curve is defined as leptokurtic, that is, more "pointed" than a normal distributed one. < 3 the curve is defined as platykurtic, i.e. more "flat" than a normal distributed one. It is calculated using the Matlab function `kurtosis(x)`.

- *Maximum and Minimum:* the minimum and the maximum value of the amplitude of the signal in the time domain.

- *Position of Maximum and Minimum:* index of the sample in which the maximum and minimum value of the amplitude of the signal is recorded. In each trial of thinking period, the samples are numbered from 1 to L

- *Area Under the Curve:* evaluated using the Matlab function `trapz(x)`, which computes the approximate integral of x via the trapezoidal method with unit spacing.

- *Number of Peaks:* number of local maximum of the signal. A local maximum is a sample which larger than its two neighboring samples. It is evaluated with the Matlab function `findpeaks(x)`

- *Peaks Mean:* mean of the value of the local maximum of the signal.

Range Features

Range features also characterize the EEG signals in the time domain, but, instead of considering the signal as a time-series of measure, a new vector is obtained from the peak to peak measure of the voltage. This new signal, named rangeEEG, is calculated over a short-time windowed segment as the difference between the maximum and minimum:

$$rEEG_i[l] = max(x_i[n]w[n - lK]) - min(x_i[n]w[n - lK]) \tag{2.3}$$

$w[n]$ is the Hamming window used. The length of the window, M, is 1/5 of the length of the segment x, N. K is the time-shift factor, related to the percentage overlap H, set at 50, and window length M as $K = [M(1 - H/100)]$. To represent the range EEG, the following features are used:

- *Mean:* mean value of the range EEG. It is evaluated with the Matlab function `nanmean(rEEG)`, which calculates the mean of rEEG after removing the NaN values.

- *Standard Deviation:* as for the amplitude features, evaluated with Matlab as `nanstd(rEEG)`

- *Coefficient of Variation:* is the ratio between the standard deviation and the mean, as evaluated above.

- *Median:* evaluated with the Matlab function `nanmedian(rEEG)` which returns the sample median of the range eeg, treating NaNs as missing values.

- *Lower and Upper Margin:* are evaluated as the 5th 95th percentiles respectively and represented in the following as R_{lower} and R_{upper} They are calculated in Matlab as R_{lower} = `percentile(rEEG, 5)` and R_{upper} = `percentile(rEEG, 95)`

- *Width:* is a measure of the spread og the rEEG. It calculated as the difference between the upper and lower margin:

$$R_{width} = R_{upper} - R_{lower} \tag{2.4}$$

.

- *Asymmetry:* is a mesure of the symmetry of the rEEG and it's calculated as:

$$R_{asymm} = \frac{(R_{upper} - R_{median}) - (R_{median} - R_{lower})}{R_{width}} \tag{2.5}$$

R_{asymm} ranges from -1 to 1; values close to 0 indicate symmetry and values close to $\pm$ 1 indicate asymmetry of the rEEG

Spectral Features

These features represent the spectral characteristics of the signals. The first step to evaluate all the spectral features is to estimate the power spectral density (PSD) of each segment of the EEG signals, $x[n]$, of length N (approximately 10 seconds/5000 samples).

The PSD estimate used is the Welch priodogram $P_x[K]$:

$$P_x[k] = \frac{1}{LMU} \sum_{l=0}^{L-1} | \sum_{n=0}^{M-1} x[n]w[n - lK] * e^{-j2\pi kn/M}|^2 \tag{2.6}$$

where $w[m]$ is the analysis window of length M with energy U, a Hamming window is used; K is the time shift factor related to the percentage overlap H and to the window length M as $K = [M(1 - H/100)]$; L is the number of segments obtained with the windowing: $L = [(N + K - M)/K]$

In particular, the PSD is estimated using the matlab function `pwelch`, with the following options:

Window type: Hamming
Window length (M): 1/2 of the length of $x[n]$
Overlap percentage: 50
Number of DFT points: 5000 (If it is greater than the segment length, the data is zero-padded)

The features used for describing the signals in the frequency domain are listed below; P_x is the PSD estimate.

- *Power:* calculated as the area under the curve delineated by P_x, in matlab `trapz(Px)`.
- *Mean:* mean of the values in P_x
- *Number of Peaks:* number of local maximum (as defined for the amplitude feature) in the power spectrum Px. The number of peaks is quantified using the Matlab function `findpeaks(Px)`.
- *Peaks Mean:* mean of the value of the local maximum of P_x.
- *Maximum and Minimum:* values of the absolute maximum and minimum of P_x.
- *Position of Maximum and Minimum:* index of the frequency at which the maximum and minimum value of the amplitude of P_x is recorded.
- *Flatness:* also known as Wiener entropy, is a measure of the width and uniformity of the power spectrum. It is estimated using:

$$F_{wiener} = \frac{\exp\left(\frac{1}{L}\sum_{k=a}^{b}\log P_x[k]\right)}{\frac{1}{L}\sum_{k=a}^{b}\log P_x[k]} \tag{2.7}$$

where L is the length of the sequence $[a, b]$ representing the range of the frequency band.

– *Entropy:* also known as Shannon entropy, quantifies the global regularity of the power spectrum. It is estimated using:

$$F_{shannon} = -\frac{1}{\log L} \sum_{k=a}^{b} \bar{P}x[k] \log \bar{P}_x[k] \tag{2.8}$$

where $\bar{P}x$ is calculates as $\bar{P}_x = P_x[k] / \sum_{k=a}^{b} P_x[k]$

2.5.2 fNIRS features

In the following, the vector containing the N samples of one thinking period recorded in one channel is indicated with y. The features extracted from the fNIRS signals are:

– *Mean:* is the mean of the signal in the time domain.

– *Variance:* expected value of the squared deviation from the mean of y. It is quantified using the Matlab function `var(y)`.

– *Maximum and Minimum:* values of the absolute maximum and minimum of y.

– *Skewness:* measure of the degree of asymmetry of the distribution of the data around the mean value. As for the EEG signals, it is evaluated using the Matlab function `skewness(y)`.

– *Kurtosis:* it is an index of the Gaussianity of the data distribution. As for the EEG signals, it is calculated using the Matlab function `kurtosis(y)`.

– *Root Mean Squared:* is defined as the square root of the mean square, i.e. the arithmetic mean of the squares of a set of numbers and it is a measure of the magnitude of the data. It is estimated using the Matlab function `rms(y)`.

– *Slope:* the data in the vector are fitted using a 1st order polynomial: $y[n] = P(1) * n + P(2)$. The coefficients of the polynomial are estimated using the Matlab function `polyfit(t, y, 1)`, where t is a vector containing the istants of sampling. The first coefficient ($P(1)$) is considered as the features Slope.

– *Polynomial Slope:* the data in the vector y are fitted using a polynomial of degree 4: $y[n] = P(1) * n^4 + P(2) * n^3 + P(3) * n^2 + P(4) * n + P(5)$. The first coefficient ($P(1)$) is considered as the features Polynomial Slope.

2.6 Features Selection

After the features extraction phase, regardless of the type of signal that has been processed (EEG only, NIRS only, both), hundreds of variables are obtained that could potentially be used for classification. The high dimensionality of the data often decreases the ability of learning algorithms to extract useful information and correctly classify the classes.

Feature selection is the process of identifying a subset of relevant features that are the most suitable to distinguish the classes and it is necessary mainly for three reasons:

1. *Improving of classifier generalization:* generalization is a kind of ability with which a learned model can obtain good prediction results on unseen data. Learning unknown models from a high-dimensional feature space runs the risk of overfitting leading to poor generalization and consequently bad classification performances. [34]

2. *Removing irrelevant and dependent variables:* a feature can be regarded as irrelevant if it is conditionally independent of the class labels. To remove an irrelevant feature, a feature selection criterion is required which can measure the relevance of each feature with the output class/labels. [35]

3. *Reducing the effect of noise:* the data collected is often contaminated by a lot of noise. Although in the filtering phase much of the noise is removed, some components may

remain in the signals and some of the extracted features, although theoretically relevant for classification, may reflect these components instead of the useful information, degrading learning abilities.

Hence, some procedure to evaluate, rank and eventually remove the features must be adopted to obtain a subset of features. The features selection methods can be divided into three categories: [36]

1. *Filter methods:* use different techniques to rank the features according to some properties (i.e relevance); the highly ranked features or the features above a certain threshold are selected and applied to a predictor.

2. *Wrapped Methods:* the selection criterion is the performance of the predictor using a subset of features. Since directly evaluating all the subsets of features for a given dataset becomes a hard or even infeasible problem in terms of computational costs, suboptimal subsets are found by employing search algorithms.

3. *Embedded methods:* a trade-off between the first two methods by embedding the feature selection into the model construction. Embedded methods select features during the process of model construction to perform feature selection without further evaluation of the features.

In this work, a wrapped method is used: several subsets of features are created and the one where the classifier has better performance is chosen.

The subsets of features are first created by choosing the features extracted from the signals of the n_c channels ranked as most informative; then the number of features is further reduced by choosing, for EEG signals, the features of the most n_b informative frequency bands, while for fNIRS signals the features of the signal types (oxy/doxy) ranked as most informative. The following sections 2.6.1 and 2.6.2 explain how the channels, bands and types of signals are sorted.

After the selection of channels, bands, and signal types the number of features is further reduced: features belonging to the selected n_c channels and n_b bands/types are ranked using

the Maximum Relevance Minimum Redundancy (mRMR) method (see 2.6.3) and the first n_f features are used to the learning process of the classifier.

A remaining issue is how to determine the optimal number of channels n_c, of bands/types n_b, and features n_f to use to create the optimal subset of features. For this reason, many subsets of features are created, varying the number of channels n_c, the number of frequency bands/types of signal n_b and, finally, the number of features used n_f. The different subsets thus created are used to train and test as many classifiers. (See Section 2.7 for classifiers description). Then the subset of features is chosen whose corresponding classifier has obtained the best performance in prediction. If two subsets lead to the same accuracy, the one with the lowest number of features is chosen to reduce the computational cost.

Before using any features ranking or selection method, features are normalized by subtracting the mean and dividing by the standard deviation.

2.6.1 Channels selection

Some of the channels used for the acquisition of signals, both EEG and fNIRS, sometimes, due to their position or to some malfunction, do not bring any useful information to the classification. For this reason, the channels are ranked on the basis of their mutual information with the class labels. The channel selection is treated as a features selection problem, considering all features coming from a channel together; in particular, the mutual information between the set of features extracted from a channel and the class labels is estimated: $[I_1(x_{c1}, c)$, $I_2(x_{c2}, c)$,..., $I_d(x_{cd}, c)]$. x_{c1} is the set of features extracted by the signals of channel 1, c are the class labels and d is the number of channels. [37]

Only the features belonging to the n_c channels with the higher mutual information will pass to the selection phases described in the next sections 2.6.2 and 2.6.3. The number of channels selected n_c varies across the different features subsets.

2.6.2 Bands and type selection

The selection of the bands (EEG signals) and of the types of signals (fNIRS signals) happens exactly in the same way as the selection of the channels but, the mutual information is calculated between the class labels and blocks of features that have in common the frequency band or the type of signals from which they have been extracted.

The number of bands/signal types selected n_b varies across the different features subsets.

2.6.3 Features ranking

The features contained in each subset created with the channel and band/type selection are still some tens. Some of them could be redundant, correlated or irrelevant, undesirable characteristics for the features to be used in the prediction process since adding no information but just noise to the prediction process.

To select the features with maximal relevance to the target class c, measures of mutual information or correlation are usually used. These methods operate a sequential search, ranking the features with a score and selecting the n_f best individual features. Though "the n_f best features are not the best n_f features": it is likely that features selected according to Max-Relevance could have large redundancy. When two features highly depend on each other, the respective class-discriminative power would not change much if one of them were removed, but, oppositely, there would be less probability of over-fitting and addition of noise. So, in this final phase of features selection, the Max-Relevance, Min-Redundancy (mRMR) method is applied to have mutually exclusive and relevant features. [38]

In mRMR method, features are subsequently added to the new subset to maximize the operator $\Phi(D, R) = D - R$ where D represent the relevance of a features and is obtained with

$$D = \frac{1}{|S|} \sum_{x_i \in S} I(x_i, c) \tag{2.9}$$

and R, representing the redundancy factor, with

$$R = \frac{1}{|S|^2} \sum_{x_i, x_j \in S} I(x_i, x_j) \tag{2.10}$$

$I(x_i, c)$, in 2.9, is the mutual information between the individual feature x_i and the class labels in c; $I(x_i, x_j)$, in 2.10, is the mutual information between the feature x_i and x_j; S is the cardinality of the subset of already selected features, x_i is the feture candidate to participate in the subset.

The operator $\Phi(D, R)$ combine the constraints of the maximal relevance criterion and minimal redundancy condition, respectively: $maxD(S, c)$ and $minR(S)$.

In practice, every feature is added to the subset of selected features when maximizes Φ until the subset has reached the maximum desired cardinality n_f.

This features selection method has been implemented by adapting the code proposed in the Matlab toolbox "FSLib 2018" developed by Roffo et al.[39] [40]

2.7 Classification

For the classification task, a support vector machine (SVM) model is used. The classifier is built using the Matlab `fitcsvm` which trains an SVM model for two-class classification on a low-dimensional predictor data set with automatic parameter optimization obtained setting the 'OptimizeHyperparameters' option as 'auto'. For more robust results, 5-fold validation is used with a different partition at each iteration.

To verify that the built classifier is significantly different from a random one, the chance level with a confidence interval at $\alpha = 0.05$ was calculated as proposed by Müller-Putz et al. in [41]. Indeed, it is not only meaningful to present classification accuracies, but also the number of trials on which the computations are based. Exemplarily, the chance level in a simple 2-class paradigm is not exactly 50%; more precisely, it is 50% with a confidence interval

at a certain level α depending on the number of trials. The confidence intervals are given by

$$p \pm \sqrt{\frac{p(1-p)}{n+4}} Z_{(1-\frac{\alpha}{2})} \tag{2.11}$$

where p is the theoretical chance level and, since both classes are equally likely to occur; $p = 0.5$; n is the number of trials used to evaluate the accuracy; $Z_{(1-\frac{\alpha}{2})}$ is the $1 - \frac{\alpha}{2}$ quantile of the standard normal distribution.

2.8 Offline Analysis method

The offline analysis is carried out considering the blocks acquired during the same session.

The blocks are initially processed all together and then, before extracting features, the signals are divided into two parts, train and test set, considering the chronological order of acquisition. In all the offline analysis, 2/3 of the thinking period signals compose the train test and the remaining 1/3 is used for the test set.

From the first set of signals, all the available features are extracted and normalized (i.e. mean subtraction and division for the standard deviation), saving the parameters (mean and standard deviation) used for the normalization which will be used on the test set to simulate the online procedure. These features are then passed to the selection process.

As explained in the sections 2.6.1, 2.6.2 and 2.6.3, the subsets to be tested are created first by varying the number of channels chosen n_c from 1 to 5, and then varying the number of bands/types n_b from 1 to 3 (for fNIRS signals, there being only 2 different types, the number varies from 1 to 2), obtaining $n_b * n_c$ different subsets. The n_i features contained in each of these $n_b * n_c$ subsets are now ranked with the mRMR method and the final subsets to be tested are created by varying from 1 to ni/2 the number of features chosen from the best ranked.

Once obtained many subsets of features, to choose the best one for predicting, there is a further random subdivision to evaluate the performance of the classifier: each subset of

features is again divided into a sub-train (70%) and a validation (30%) set. The sub-train set is used to train the classifier and built the model which is then used to predict the samples in the validation set and thus have an estimate of the accuracy. This operation is repeated several times (200) generating randomly different subdivisions of sub-train and validation set. The accuracies obtained using the different pairs of sub-train/validation sets from the same subset of features are averaged to have a stable estimate of performance. The subset which obtains the best accuracy in this phase is then selected as the (sub-)optimal one.

Subsequently, the chosen features are extracted from the test set signals and normalized using the mean and standard deviation calculated on the train set.

The model is built with the optimal subset of features using the 2/3 of the signals as the train set, on which the accuracy of the model is evaluated and the remaining 1/3 as the test set, trying to predict the labels as in the online application and evaluating the performances.

The offline analysis was carried out using:

1. only the features extracted from the EEG signals;
2. only the features extracted from the fNIRS signals;
3. the features extracted from both signals at the same time.

In the latter case, the train set is obtained by concatenating the features extracted from the EEG and fNIRS signals and then using the features selection as explained in Section 2.6.

3

Results

3.1 Signals Processing

The goal of this phase is to remove noise and artifacts that always affect the signals but, at the same time, preserve the information.

In Figure 3.1, the effect of subtracting the mean from the EEG, EMG and EOG signals can be assessed. After this operation, the signals maintain their characteristics intact and they are more easily comparable with each other. The choice to bring the signal to null average and not to normalize it (bring it to unitary variance) was made to better preserve the amplitude of peaks that could be decisive in the classification.

In the Figure 3.2, a yes and a no response sample are plotted. In both cases, the signal width is almost 20 times smaller in the Beta band than in the Delta band. In general, therefore, the filtered signal in the wideband mainly reflects the components of the two slowest bands, Delta and Theta, while the two fastest bands provide little information, as expected from the

physiological characteristics of the EEG signals of this patient.

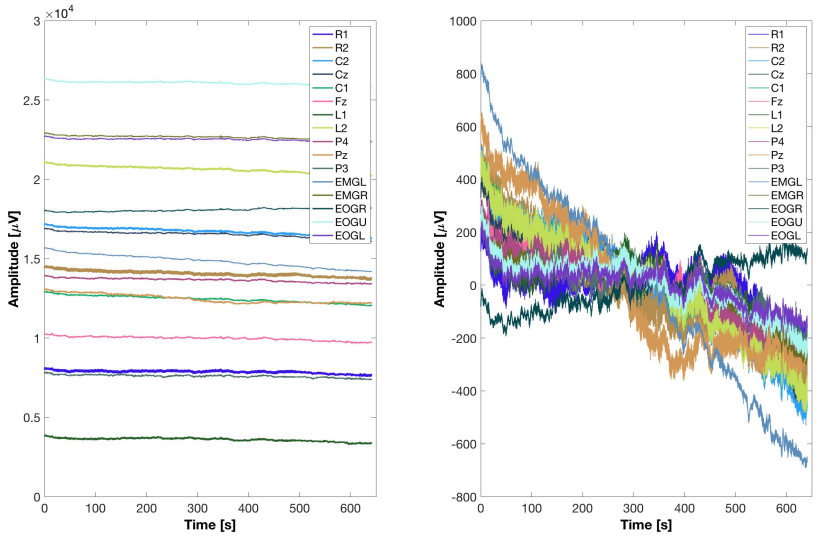

Figure 3.1: *EEG, EOG and EMG signals before and after mean subtraction:*
The plots show a fraction (700s) of the signals acquired from 5 EEG, 4 EMG and 4 EOG channels during a training block (in particular visit 1, day 1, block 1). The raw signals, as acquired from the amplifier are plotted on the left while, on the right side, there are the same signals after the mean subtraction.

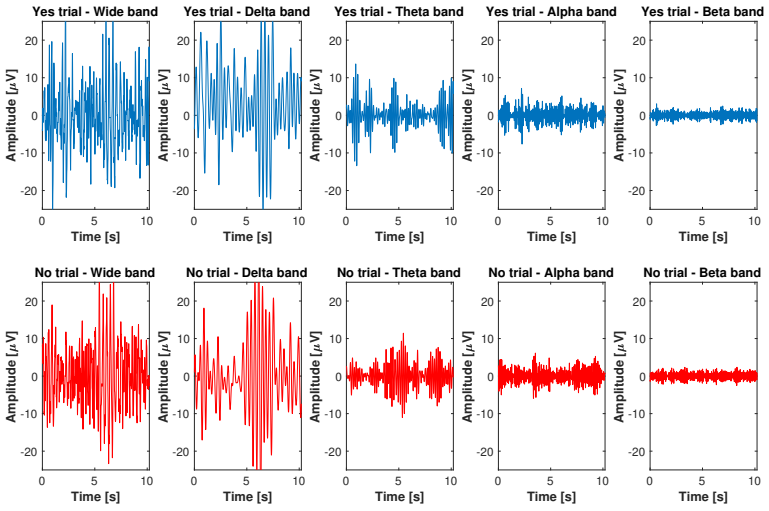

Figure 3.2: *EEG Yes and No signals filtered in 5 bands*
Example of two segments of EEG signal, representing one yes thinking period (above) and one no thinking period (below), filtered and divided in the 5 bands of interest. The signals plotted are form channel Cz, extracted from block 4 of visit 7, day 3

Figure 3.3: *EEG, EMG and EOG before and after processing*
The signal represents the first thinking period acquired in an EEG (Cz), EMG (EMGL) and EOG (EOGR) channel of visit7, Day3, block 4. Each of the signals is plotted as acquired (1), after the mean subtraction (2) and after the band-pass filtering (3)

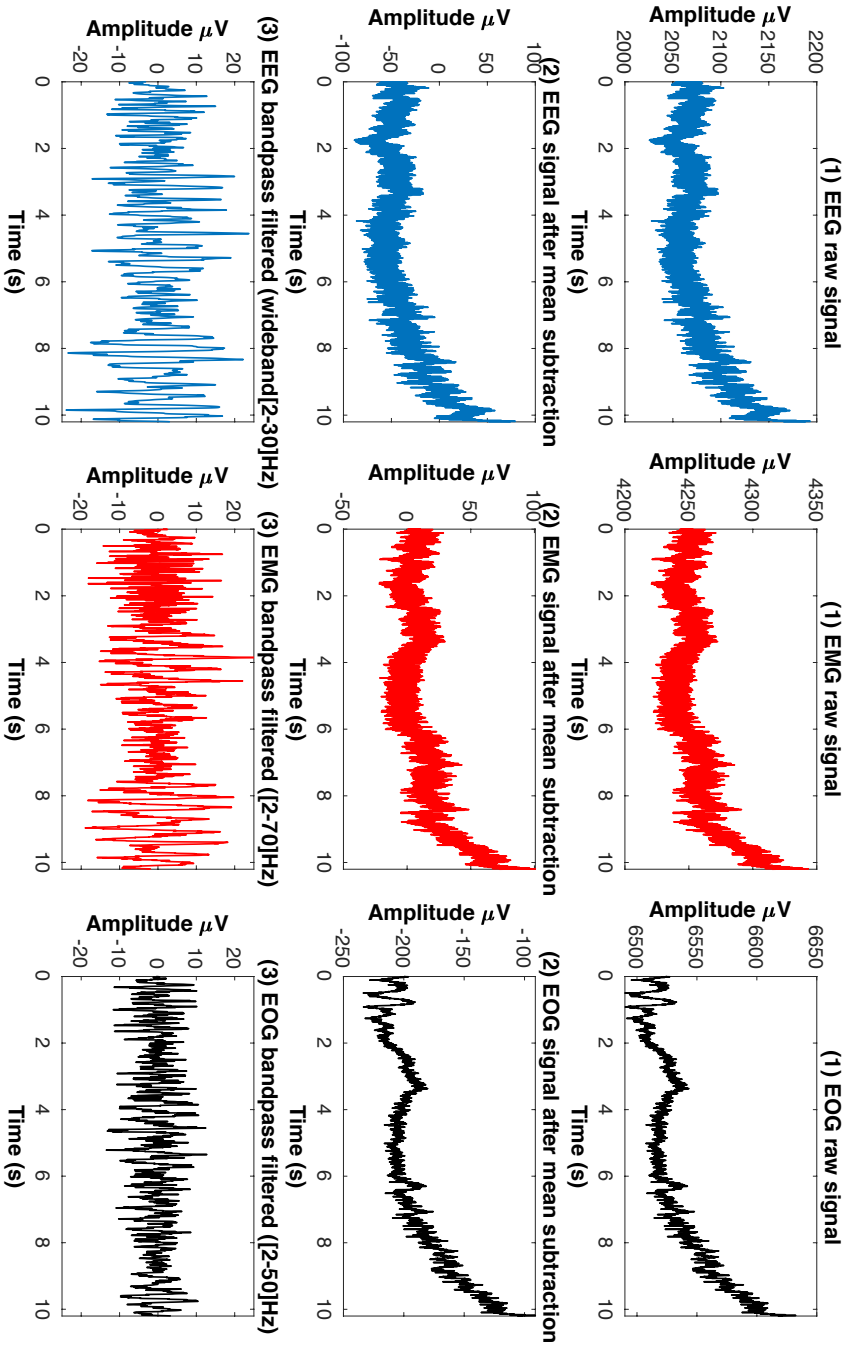

In Figure 3.3, the main phases of the processing are shown for EEG, EMG and EOG signals. Bandpass filtering removes the fastest components of the signal which, considering the physiological characteristics of the brain activity of patients with ALS, are attributable only to noise. With this operation, as it is clearly seen in the figure 3.3, also the drift of the signals, attributable to artifacts caused by the instrumentation, is removed.

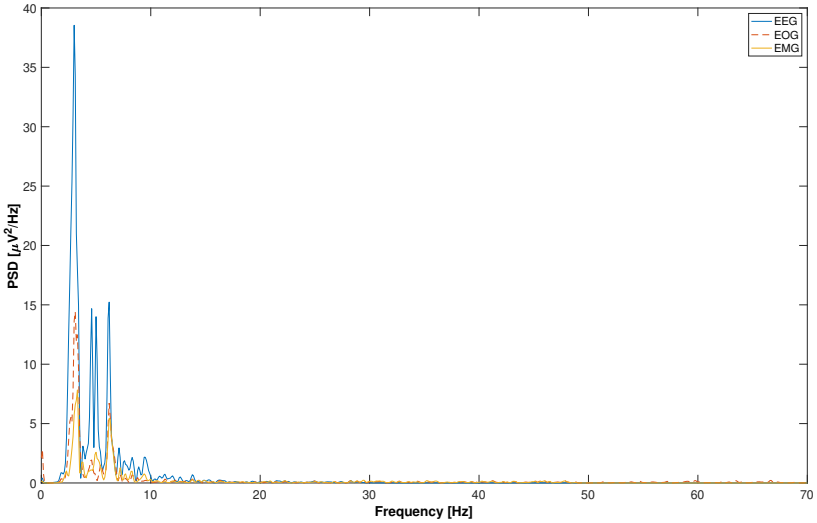

Figure 3.4: *Power Spectrum of EEG, EOG and EMG signals:* Plot in the window [0-70Hz] of the PSD of the first thinking period acquired in a EEG (Cz), EMG (EMGL) and EOG (EOGR) channel of visit7, Day3, block 4.

The spectral analysis of the EEG, EOG and EMG signals, of which a visual example is plotted in Figure 3.4, leads to the exclusion of the EOG and EMG signals from the following phases. These signals are mainly acquired to verify if there is some residual muscular activity that can be used to differentiate between affirmative and negative responses, for example by asking the patient to move a muscle to answer yes and do nothing to answer no. In this case, the activity by EMG and EOG is too slow and weak to be traced back to voluntary muscle activity. Including these signals in the following phases of features extraction and selection would lead to include signals that are not very informative but noisy.

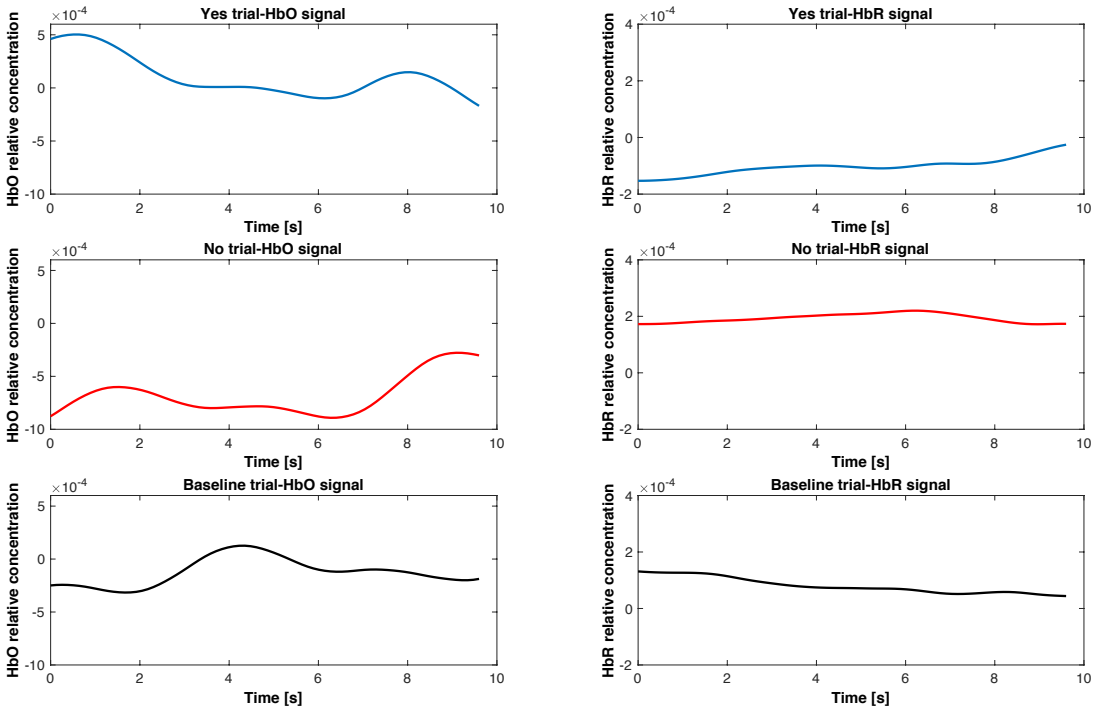

Figure 3.5: *HbO and HbR fNIRS Yes and No signals*
Example of two segments of fNIRS signals, representing one yes thinking period (above) and one no thinking period (below). The signals on the left are the measure of the relative changes in the concentration of HbO, while the signals on the right are the measure of the relative changes in the concentration of HbR. The signals plotted are recorded from the same channel, extracted from block 4 of visit 7, day 4

The Figure 3.5 shows three fNIRS signal segments once fully processed and obtained the relative concentrations of HbO and HbR. The three segments represent a yes response period, a no response period and a baseline period. There is a considerable difference in the amplitude of the HbO and HbR signals.

3.2 Features Extraction and Selection

From the acquired EEG or fNIRS signals, the features, used in the following phases of model construction and prediction, are extracted. EEG and fNIRS signals are treated separately respecting their different physiological nature, as explained in Section 2.5.1 and 2.5.2.

The extracted features are organized in $n_t \times n_f$ matrices where n_t is the number of trials

considers and n_f is the number of features extracted.

3.2.1 Features extracted from EEG signals

Initially $n_{f_{tot}} \times n_{c_{tot}} \times n_{b_{tot}}$ features are extracted from each EEG thinking period signal in the train and validation sets, where $n_{f_{tot}} = 29$ is the total number of available features for EEG signals; $n_{c_{tot}}$ is the total number of EEG acquisition channels which varies among the different visits and is reported in 2.1; and $n_{b_{tot}} = 5$ is the number of frequency band in which the signals are filtered (Wide band, Delta band, Theta Band, Beta Band, and Alpha Band). The following Tables show the number of channels, bands and features chosen to obtain the (sub)optimal subset of features extracted from EEG signals for classification in each session.

Session	N° of blocks	Validation Accuracy (%)	n_c	n_b	n_f
Day 1	2	87.00	2	3	73
Day 2	4	70,437	1	1	8
Day 3	2	91.250	1	2	6
Day 4	3	84.833	5	3	97
Day 5	2	86.375	3	2	5
Day 6	4	66,562	5	3	47

Table 3.1: *Selection of features extracted from the EEG signals of visit1*

Session	N° of blocks	Validation Accuracy (%)	n_c	n_b	n_f
Day 1	5	70.55	4	1	1
Day 2	4	72.063	2	2	10
Day 3	1	90	2	2	1

Table 3.2: *Selection of features extracted from the EEG signals of visit5*

Session	N° of blocks	Validation Accuracy (%)	n_c	n_b	n_f
Day 1	2	64.250	1	3	14
Day 2	3	79.5	3	2	3
Day 3	4	79.125	5	3	14
Day 4	5	68.250	2	3	12
Day 5	4	70.937	1	1	3

Table 3.3: *Selection of features extracted from the EEG signals of visit6*

Session	N° of blocks	Validation Accuracy (%)	n_c	n_b	n_f
Day 1	3	71.334	2	1	3
Day 2	4	63.5	2	3	13
Day 3	3	73.312	5	1	3
Day 4	4	75.812	3	3	54

Table 3.4: *Selection of features extracted from the EEG signals of visit7*

3.2.2 Features extracted from fNIRS signals

Initially $n_{f_{tot}} \times n_{c_{tot}} \times n_{t_{tot}} = 440$ features are extracted from each fNIRS thinking period signal in the train and validation sets, where $n_{f_{tot}} = 11$ is the total number of available features for fNIRS signals; $n_{c_{tot}} = 20$ is the total number of fNIRS acquisition channels; $n_{t_{tot}} = 2$ is the number of different types of fNIRS signals reconstructed (oxy/dxy). The following Tables show the number of channels, type of signal and features chosen to obtain the (sub)optimal subset of features extracted from fNIRS signals for classification in each session.

Session	N° of blocks	Validation Accuracy (%)	n_c	n_b	n_f
Day 1	2	77.5	4	1	24
Day 2	4	68.187	5	1	28
Day 3	1	92.25	4	1	7
Day 4	3	72.5	4	2	1
Day 5	2	73.125	5	2	8
Day 6	4	67.5	4	1	11

Table 3.5: *Selection of features extracted from the fNIRS signals of visit1*

Session	N° of blocks	Validation Accuracy (%)	n_c	n_b	n_f
Day 3	4	64.875	5	2	26

Table 3.6: *Selection of features extracted from the fNIRS signals of visit5*

Session	N° of blocks	Validation Accuracy (%)	n_c	n_b	n_f
Day 1	2	83.125	4	1	1
Day 2	3	60.2	2	1	10
Day 3	4	64.625	5	2	26
Day 4	5	74.437	5	1	2
Day 5	4	74.625	5	2	13

Table 3.7: *Selection of features extracted from the fNIRS signals of visit6*

Session	N° of blocks	Validation Accuracy (%)	n_c	n_b	n_f
Day 1	2	83.125	4	1	1
Day 2	3	60.2	2	1	10
Day 3	4	64.625	5	2	26
Day 4	5	74.437	5	1	2

Table 3.8: *Selection of features extracted from the fNIRS signals of visit7*

3.2.3 Combination of features extracted from EEG and fNIRS signals

Before proceeding with the combined analysis of the features extracted from EEG and fNIRS, the perfect correspondence between the blocks acquired with the two methods was checked, verifying the coincidence of the triggers and the class labels. In some cases, in fact, for various reasons, the acquisition may not have taken place with both techniques at the same time. Following these checks, the combined analysis was not possible for the sessions of visit 5 and for the Day 2 of visit 6. For the same reason, in some sessions, only fewer blocks are used than in the corresponding separate EEG and fNIRS analyses.

The combination of the features of the EEG and fNIRS signals was obtained by chaining the two matrices resulting separately from the two different extraction procedures.

The features selection then takes place in the same way as when only one type of signal is considered. The channels are sorted and if the bests are only the fNIRS acquisition channels, in the next step only the type of signals between oxy and dxy is chosen. If instead some EEG channels and some fNIRS channels are chosen at the same time, the ranking to choose n_b is made between the frequency bands and the types of signals (oxy/dxy).

Session	N° of blocks	Validation Accuracy (%)	n_c (EEG/fNIRS)	n_b	n_f
Day 1	2	78.375	5 (3/2)	3	124
Day 2	4	68.5	5 (0/5)	1	28
Day 3	1	92.5	4 (0/4)	1	13
Day 4	3	72.667	3 (0/3)	1	7
Day 5	2	73.125	5 (1/4)	3	19
Day 6	4	66.625	5 (0/5)	1	12

Table 3.9: *Selection of features extracted from the EEG and fNIRS signals of visit1*

Session	N° of blocks	Validation Accuracy (%)	n_c (EEG/fNIRS)	n_b	n_f
Day 1	2	83.75	3 (1/2)	2	1
Day 3	4	65.687	5 (0/5)	2	26
Day 4	5	75.5	5 (0/5)	1	2
Day 5	4	74.187	4 (0/4)	1	6

Table 3.10: *Selection of features extracted from the EEG and fNIRS signals of visit6* The analysis of day 2 was not possible due to mismatch of the fNIRS and EEG signal blocks

Session	N° of blocks	Validation Accuracy (%)	n_c (EEG/fNIRS)	n_b	n_f
Day 1	3	68.167	5 (2/3)	2	5
Day 2	4	67.25	3 (0/3)	1	15
Day 3	4	67,313	5 (0/5)	2	2
Day 4	3	69.375	3 (0/3)	1	4

Table 3.11: *Selection of features extracted from the EEG and fNIRS signals of visit7*

3.3 Classification

First of all, the adjusted chance levels are calculated based on the number of trials considered, as proposed in [41]. Indeed, the chance level in a 2-class paradigm is not exactly 50%, but, more precisely, it is 50% with a confidence interval at a certain level α depending on the number of trials. In particular, the chance levels calculated in the Table 3.12 using Equation 2.11 with $\alpha = 0.05$, serve to assume that, if a given classifier has prediction accuracy greater than the corresponding chance level, it differs significantly from a random one with 95% confidence.

In Table 3.12, the new estimated chance levels are shown for a correct analysis of the results of the classification reported below

N° of blocks	Test trials	Test trials/class	Chance level (95% confidence)
2	14	7	70 %
3	20	10	67 %
4	26	13	65 %
5	34	17	63 %

Table 3.12: *Adjusted chance level:*
calculated as proposed by Müller-Putz et al. in [41] on the basis of the number of trials on which the model accuracy is evaluated

In the following, "Model Accuracy" is the accuracy obtained on the train test with the validation process, while "Classification Accuracy" is the accuracy of the classifier predicting the class of the samples in the test set.

In all the cases reported below, the model accuracy is obtained with the 5-fold cross-validation on the train set while the classification accuracy is obtained using the model created with the Matlab function `traincsvm` to predict the classes of the test set.

3.3.1 Classification with EEG signals

The results obtained using only the features extracted from the EEG signals are shown below. The number of features used to create the train and test set in each session, as well as the number of blocks considered, is the one reported in the corresponding Tables 3.1, 3.2 3.3, and 3.4 of the Section 3.2.1.

The results obtained are poor with only 1 session out of 18 above the chance level.

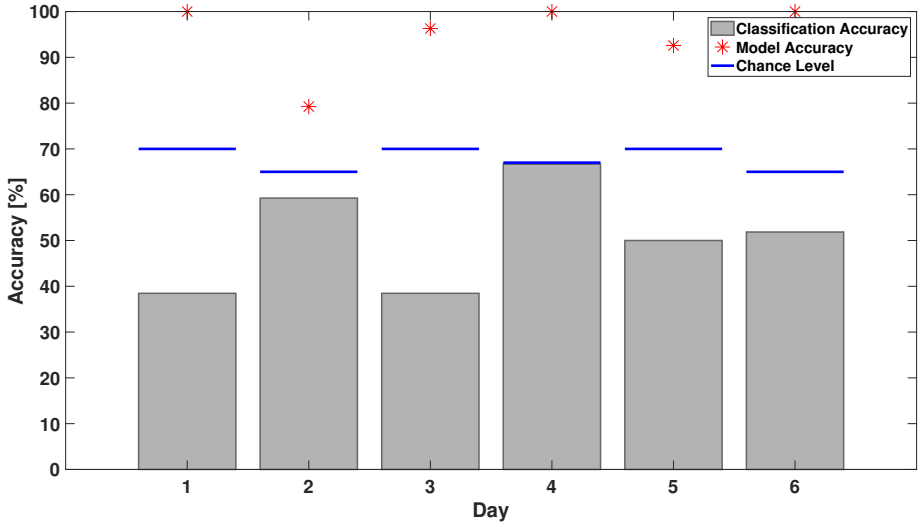

Figure 3.6: *Classification results using EEG signals for visit 1*

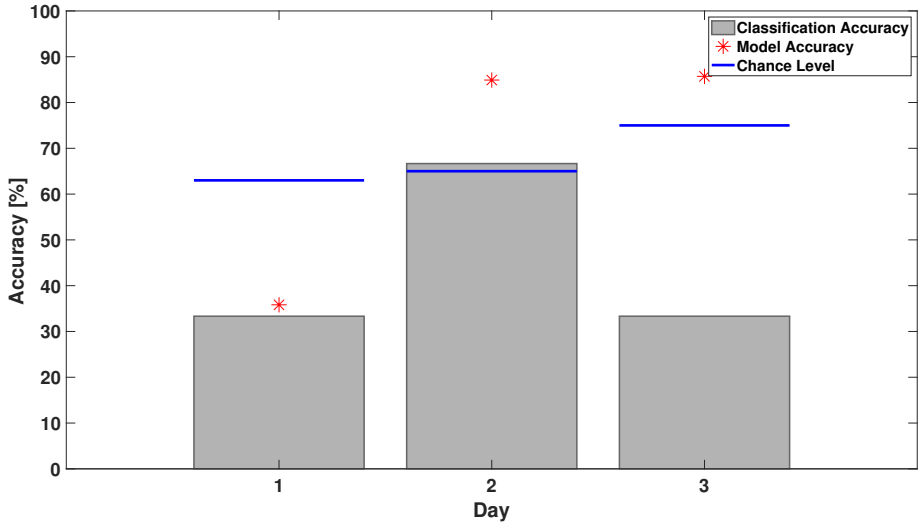

Figure 3.7: *Classification results using EEG signals for visit 5*

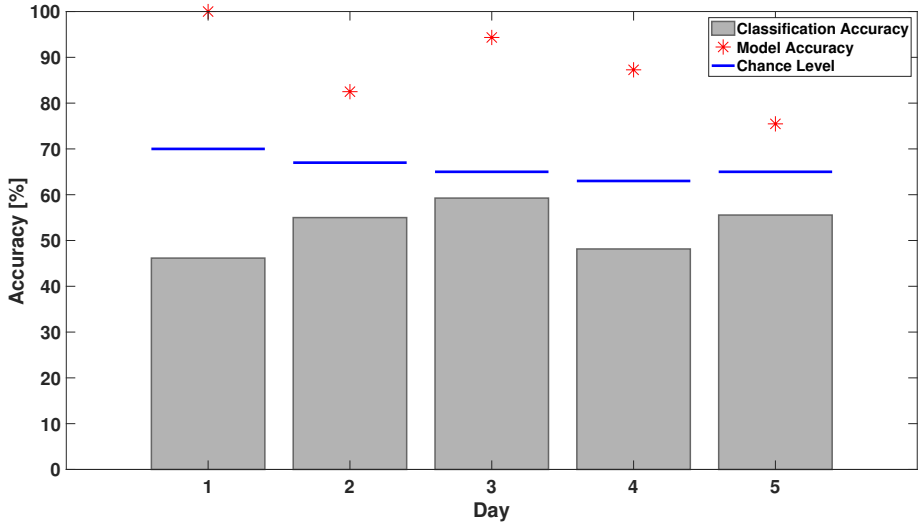

Figure 3.8: *Classification results using EEG signals for visit 6*

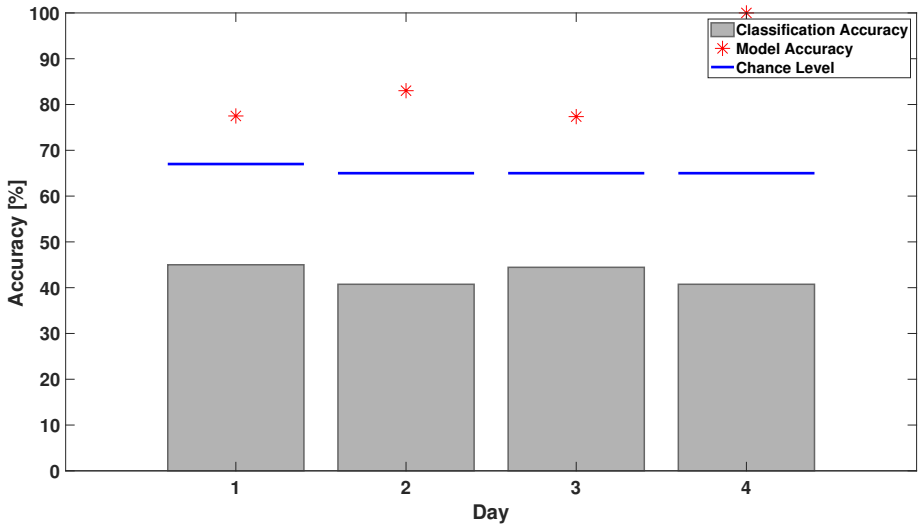

Figure 3.9: *Classification results using EEG signals for visit 7*

3.3.2 Classification with fNIRS signals

The results obtained using only the features extracted from the fNIRS signals are shown below. The number of features used to create the train and test set in each session, as well as the number of blocks considered, is the one reported in the corresponding Tables 3.5 3.6 3.7, and 3.8 of the Section 3.2.2.

In 7 out of 16 sessions analyzed it was possible to predict the thinking period signal class using the features extracted from the fNIRS signals with an accuracy above the chance level.

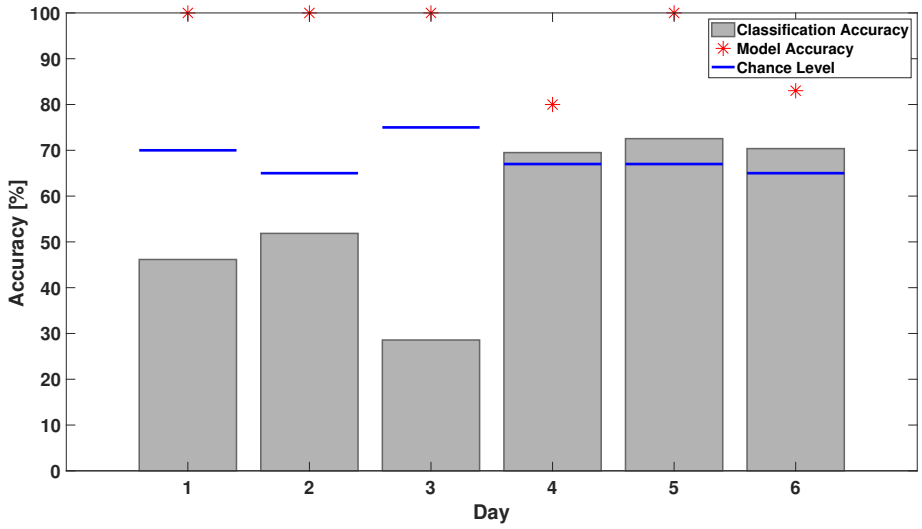

Figure 3.10: *Classification results using fNIRS signals for visit 1*

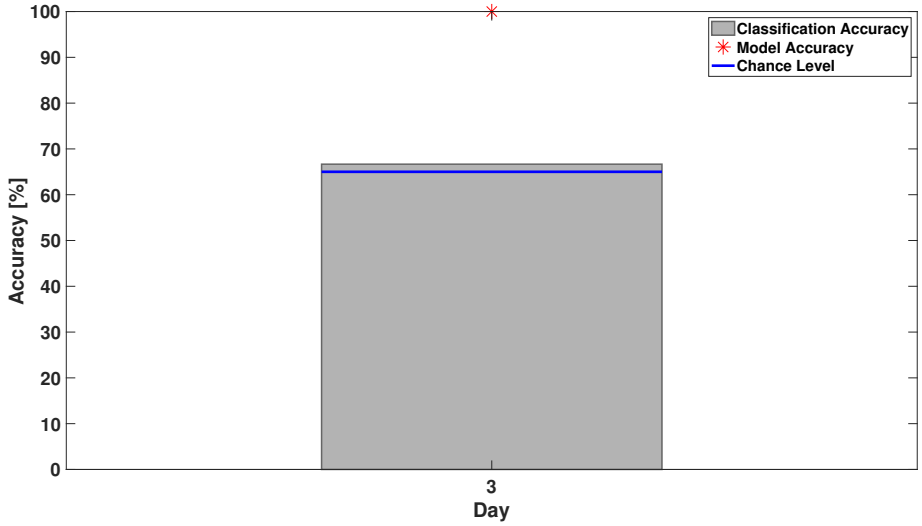

Figure 3.11: *Classification results using fNIRS signals for visit 5*

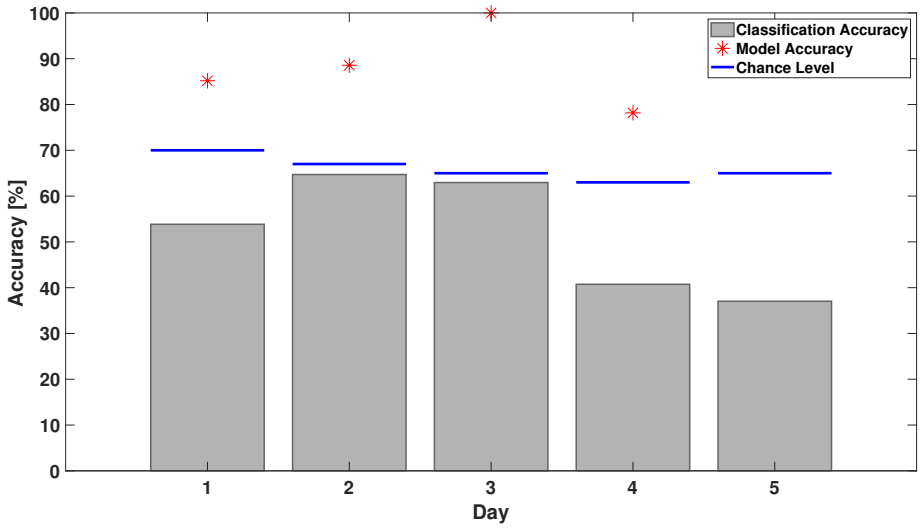

Figure 3.12: *Classification results using fNIRS signals for visit 6*

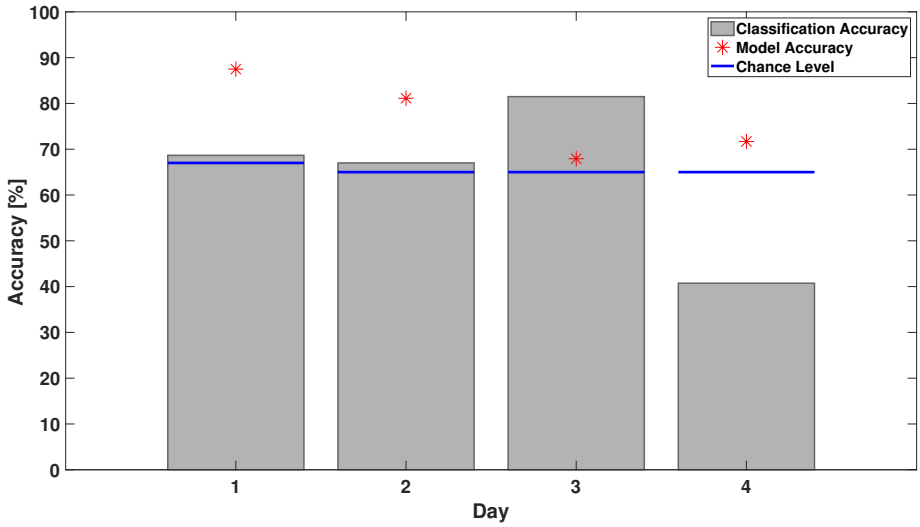

Figure 3.13: *Classification results using fNIRS signals for visit 7*

3.3.3 Classification with EEG and fNIRS signals

The results obtained by concatenating the features extracted from the EEG and fNIRS signals before selecting the features are shown below. The number of features used to create

the train and test set in each session, as well as the number of blocks considered, is the one reported in the corresponding Tables 3.9, 3.10, and 3.11 of the Section 3.2.3.

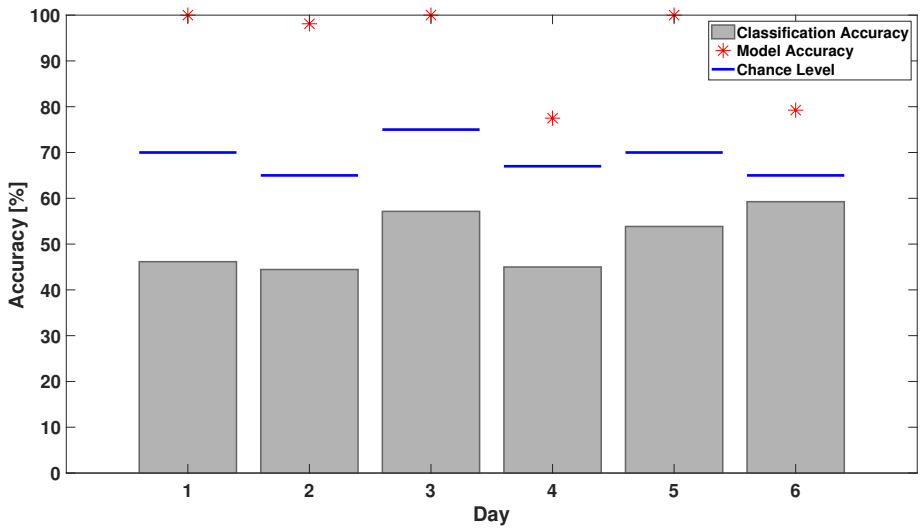

Figure 3.14: *Classification results using combination of features from EEG and fNIRS signals for visit 1*

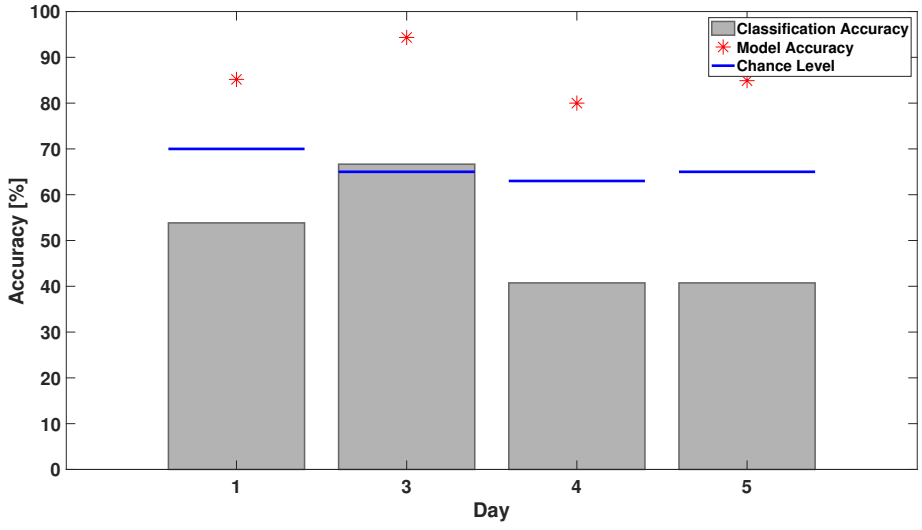

Figure 3.15: *Classification results using combination of features from EEG and fNIRS signals for visit 6*

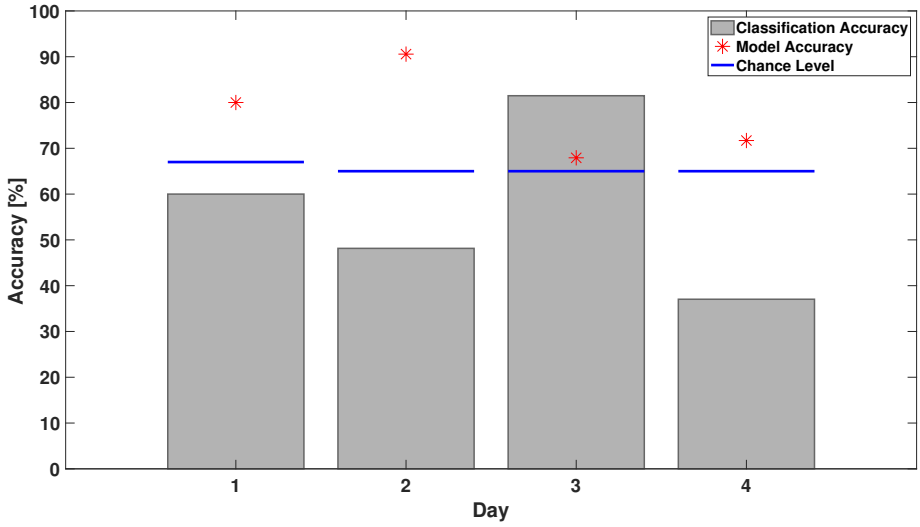

Figure 3.16: *Classification results using combination of features from EEG and fNIRS signals for visit 7*

4

Discussion

4.1 Considerations on the psychophysical condition of the patient during the visits

Classifying the signs of the thinking period following a yes or no answer to a question is a particularly difficult task when working with CLIS patients even for reasons beyond mathematical considerations. The lack of communication with the patient prevents any feedback regarding the state of health, wakefulness, attention, and interest of the subject, which are extremely important for the functioning of the system. When information on the state of the patient is available mainly thanks to the presence and collaboration of family members and caregivers, the interpretation of the results and of the correct functioning of the system is simpler and at the same time more complete.

In the cases considered, information on the psychophysical state of the patient is only available for visits 1 and 7.

Visit 1 was held at a time when, in some cases, the patient was still able to communicate using jaw movements that family members were capable of interpreting to understand his condition. In the first three days of acquisition of visit 1, the patient was not in good psychophysical condition, unlike the following days. The first visit was in fact held in Germany, in Tübingen. The patient, who lives in Italy, had faced a long journey that could have initially destabilized him. According to the relatives, however, after the necessary settling and rest following the trip, the patient greatly appreciates changing the environment. This trend is clearly reflected in the good performance of days 4,5 and 6 compared to the first three.

Visit 7 was held at the patient's home in September 2018. According to family members, on rare occasions, the patient was still able to move his jaw, especially in case of pain or discomfort. This type of movement probably represents an involuntary reflex but it is nevertheless useful for interpreting the subject's state.

During this visit, 4 days of acquisition were carried out: on days 1 and 2 the patient was instructed to think yes or no to answer the questions while, on days 3 and 4, the patient was instructed to think yes and try to move the jaw to say yes and think no and do nothing to say no. In the first two days of acquisitions of visit 7, sufficient performances are obtained; on day 3 when the patient received different instructions, the classification accuracy is particularly high. Even if analyzing the EMG signals acquired during day 3 there are no clear muscle activations, considering the good classification performance in that session, it can be assumed that it still exists a strong activation in the brain resulting from an attempt to move a muscle. This hypothesis is supported by the fact that the jaw muscle was the last muscle the patient was able to move voluntarily before the transition from LIS to CLIS.

In day 4, the patient was in a state of discomfort following a night of little sleep and pain communicated with movements of the jaw, and it was also necessary to stop acquisitions several times so that the caregivers could intervene to meet the primary needs of the patient. For this reason, it has been possible to evaluate the paradigm of day 3 only on one session and this does not allow to say with certainty that asking the patient to try to move a muscle is bet-

ter than just asking him to think yes or no. To confirm this hypothesis, further acquisitions already planned for the next months, would be necessary.

4.2 Classification with features from EEG signals

Observing the results reported in the histograms 3.6, 3.7, 3.8 and 3.9, in almost no case it is possible to classify the signal classes with accuracy above the chance level using the features extracted from the EEG signals. This leads to the assumption that the EEG signals are not very informative for the classification task using the paradigm presented.

By comparing the EEG signals of a healthy individual with the ones of an ALS patient, the latter are much slower and weaker due to physiological changes in brain functionality caused by the disease. As consequence, the non-invasively recorded EEG signals of ALS patients in this BCI system, further attenuated by the distance between source and receiver, could be overly attenuated and covered by noise to provide the information needed for classification.

Despite the fact that EEG signals from ALS patients are rather slow, their dynamic is still fast compared to other biological and neurological process and they immediately reflect a brain activation when it occurs. The features extracted and used for the classification are calculated on 10 seconds of thinking period EEG signal. It is likely that only a fraction of the EEG thinking period signal contains information about the response given by the subject and these are covered by the rest of the samples considered. It would, therefore, be necessary an approach that considers narrower windows, of 1 or 2 seconds, of EEG thinking period signals. In this case, the first problem to be addressed would be to identify which time window represents the patient's response, i.e. in which instant the brain activation corresponding to the patient answer occurs.

4.3 Classification with features from fNIRS signals

Unlike the classification using the features extracted from the EEG signals which did not lead to any significant results, using the features extracted from the fNIRS signals an accuracy

above the chance level was achieved for 7 sessions.

In the histograms in Figure 4.1 and 4.2 it is reported the distribution of features selected for classification respectively in all sessions and only in sessions with the accuracy above the chance level.

In both histograms, we observe first of all that all 9 different features proposed have been chosen for classification at least once. From this, it can be deduced that all the features and/or their combination contain some information useful to discriminate between yes and no answers.

In the sessions with the accuracy above the chance level, only 12 of the 20 channels available were taken into account; this could suggest a repositioning of the channels in order to map more densely the areas where there is more activity useful for classification. It is interesting to note that these 12 more informative channels are the channels positioned centrally on the scalp. The central histogram of Figure 4.1 shows that in sessions with classification below the chance level, different channels are chosen for classification than those used in sessions with good results. In these sessions, where the distinction between yes and no is probably less clear (or non-existent because the patient was not responding), the choice of channels is probably driven by the noise and overfitting of the model.

As can be deduced from the third histogram of both Figures 4.1 and 4.2, the signals of variation of concentration of HbO (oxy) and HbR (dxy) are equally informative and it is, therefore, necessary to consider them both for the choice of features.

A possible explanation why classification with fNIRS signals leads to better performance than with EEG signals is that the former have a slower dynamic. The effects measured with the fNIRS technique, i.e. the change in relative concentration of HbO and HbR, occur after brain activation and last for several seconds. The duration of 10 seconds of thinking period was chosen precisely to appreciate and record this type of response even if the subject actually performs the task required (answer the question) for a more limited time period.

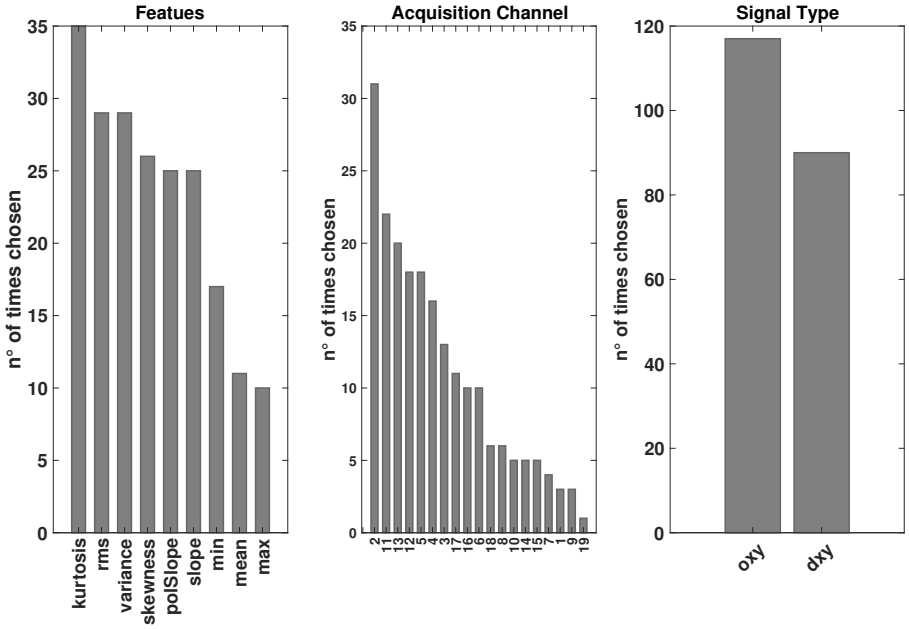

Figure 4.1: *Selected features distribution in all the sessions:*
distribution among the features typology (left), acquisition channel (center) and signal type (right) of the features selected for the classification in all the sessions considered

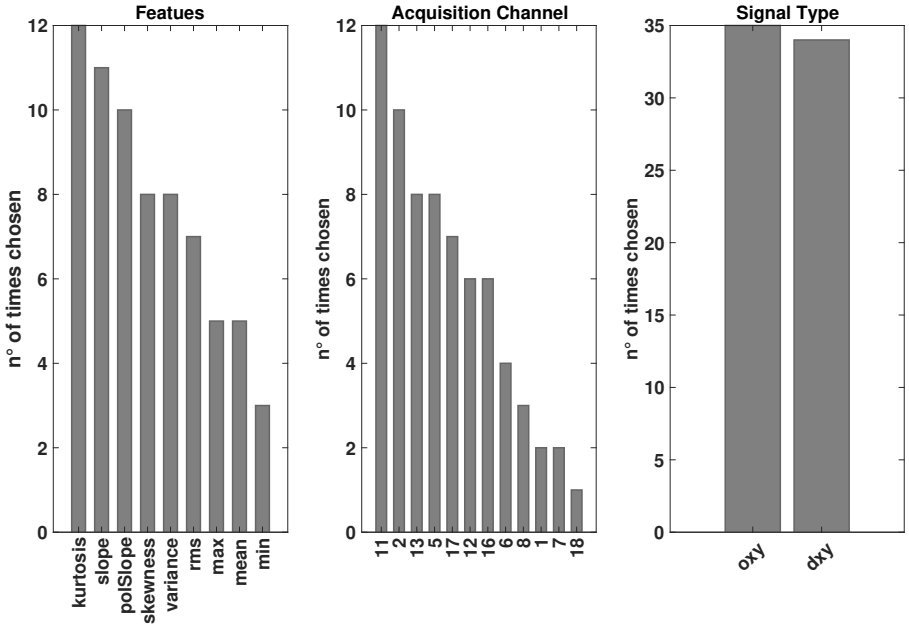

Figure 4.2: *Selected features distribution in the sessions with accuracy above the chance level:*
distribution among the features typology (left), acquisition channel (center) and signal type (right) of the features selected for the classification inthe sessions with accuracy above the chance level (i.e. visit 1,Day 4, Day 5 and Day 6; visit 5 Day 3; visit 7 Day 1, Day 2 and Day 3)

4.4 Classification with combination of features from fNIRS and EEG signals

The concatenation of the features extracted from the EEG and fNIRS signals before their selection did not lead to clear improvements in the system's performance but, on the contrary, almost in any case degraded them. This is due to the fact that the high dimensionality of the features and the small number of samples easily leads to the overfitting of the model, distorting the decision of which features are more informative than others.

On day 3 of visit 7, a session that in general has the best performance, chaining the features extracted from the EEG and fNIRS signals, exactly the same features of the case in which the selection is only among those extracted from the fNIRS signals are chosen. This means that the classifier is trained correctly and even increasing the dimensionality of the dataset with features that are not very informative (with only the EEG signals of the same session the chance level is not reached) the classifier does not go into overfitting and is able to choose the best features.

4.5 Comparison with online results

A direct comparison is possible only with the sessions of visit 7 in which the author of this work was present during the acquisitions. During the first two days of the visit, feedback sessions were done using features extracted from the EEG signals to build the model. The system of choice of features was different from the one proposed but did not lead to sufficient performance in the online classification of the signals corresponding to the thinking period.

During the day 3 feedback session was given to the patient by building the model using the fNIRS signals acquired during two training blocks. In this case, the model was built using a single function extracted on all channels and choosing one of the signals of the HbO and HbR concentration variation. The accuracy achieved online was 70%. The online system used a much simpler method for choosing features, without considering, for example, that

some channels may not be informative, that multiple features at the same time may improve performance and that both HbR and HbO can provide different information simultaneously. The development of a feature selection system that takes these considerations into account has improved performance on the same acquisition from 70% to 81.5%.

5

Conclusion

What emerges from this work is that, using the EEG signals and the proposed paradigm it is challenging to discriminate between affirmative and negative responses of the subject. Various classification approaches have been tested with the same signals leading to similar results. Several hypotheses can be advanced to explain this: recording channels in a non-invasive way, the signal already naturally weak due to the disease is excessively attenuated and covered by noise to be informative; the recorded channels are in insufficient number or in an unsuitable position; the task required from the patient and the paradigm used do not produce different brain activations for yes and no responses. However, it is important, during this BCI communication paradigm, to continue recording EEG signals from which useful information on the patient's waking state can be derived.

Using fNIRS signals instead, it is sometimes possible to obtain discreet results in the classification of yes and no answers. However, the results are not stable, making it difficult for this specific patient to communicate with open questions (with no known answer).

The combination of the EEG and fNIRS features, as proposed in this work, has not led to obvious improvements in classification performance but, on the contrary, has sometimes made it more difficult to identify the most informative features and deteriorating the results. However, it cannot be excluded that combining the two signals will not improve the performance of the system because there are several ways to explore. The combination can be done either at the level of features extraction, i.e. studying features that consider simultaneously the trend of the two signals and their correlation, or at the level of features selection, i.e. as proposed in this paper by treating the two signals separately and then concatenating their features. Without a doubt, this way will have to be taken into account in future work.

The main problem with this system is the lack of ground truth. It is impossible to say with certainty that the patient is answering all the questions and in the correct way, since he could at any time be confused, distracted or not having understood the question. To test the patient's responsiveness, for example, an option could be checking if there is a significant difference between the signal acquired in the baseline before the question and during the response period, and then not include in the process of constructing the model the thinking periods in which this difference does not occur.

Another major problem is the lack of data. During a session, in fact, it is difficult to acquire more than 4/5 blocks, corresponding to 40/50 samples per class, because each block has a duration of 12/13 minutes and prolonging the acquisitions for several hours leads to fatigue and boredom in the patient, deteriorating the results. These numbers are poor to obtain reliable statistics in the selection of features and model construction or to be able to apply more advanced and complex methods of machine learning and classification. Combining the blocks acquired in subsequent days could be a solution but even small differences in the psychophysical state of the patient would lead to false results.

Studying the trend of signals, the selected features, channels and types over time is, however, necessary way to stabilize the system. In this sense, it is essential to collect data frequently so that they are comparable with each other. The temporal distance between differ-

ent acquisitions is a concern as the patient may change the method of response and his brain activity may be markedly different due to the processes of adaptation and plasticity to which each brain is constantly subjected. This obviously requires considerable economic effort and availability of trained personnel to operate the system.

In conclusion, there are still many possibilities for study and improvement of the proposed system and it is of fundamental importance to continue this research mainly for two reasons. On the one hand, finding a stable and performing system also means better understanding the brain structure and activity in CLIS patients, fundamental information for those studying the development, diagnosis, and treatment of this syndrome. On the other hand, a system capable of restoring communication between a conscious person but unable to relate to the environment around him could greatly improve the psychological well-being of the patient himself but in the same way of his family and caregivers.

References

[1] U. Chaudhary, B. Xia, S. Silvoni, L. Cohen, and N. Birbaumer, "Brain-computer interface-based communication in the completely locked-in state." *PLOS Biology*, vol. 15, 2017.

[2] N. Birbaumer and U. Chaudhary, "Learning from brain control: clinical application of brain–computer interfaces." *Neuroforum*, 2015.

[3] J. R. Wolpaw, N. Birbaumer, W. J. Heetderks, D. J. McFarland, P. H. Peckham, G. Schalk, E. Donchin, L. A. Quatrano, C. J. Robinson, and T. M. Vaughan, "Brain–computer interface technology: A review of the first international meeting." *IEEE transaction on Rehabilitation Engineering*, vol. 8, no. 2, pp. 164–173, 2000.

[4] M. J. Aminoff, *Electroencephalography: General Principles and Clinical Applications.*, Elsevier, Ed., 2005.

[5] F. F. Jobsis, "Noninvasive infrared monitoring of cerebral and myocardial sufficiency and circulatory parameters." *Science*, no. 198, pp. 1264–1267, 1997.

[6] M. Cope, D. Delpy, E. O. R. Reynolds, S. Wray, J. Wyatt, and P. Van der Zee, "Methods of quantitating cerebral near infrared spectroscopy data." *Advances in Experimental Medicine and Biology*, no. 222, pp. 183–189, 1987.

[7] K. F. Palmer and D. Williams, "Optical properties of water in the near infrared." *Journal of the Optical Society of America*, no. 64, pp. 1107, 1110, 1974.

[8] S. Wray, M. Cope, D. T. Delpy, J. S. Wyatt, and E. O. R. Reynolds, "Characterization of the near infrared absorption spectra of cytochrome aa3 and haemoglobin for the non-invasive monitoring of cerebral oxygenation." *Biochimica et biophysica acta*, no. 933, pp. 184–192, 1988.

[9] P. W. McCormick, M. Stewart, G. Lewis, M. Dujovny, and J. I. Ausman, "Intracerebral penetration of infrared light: technical note." *Journal of Neurosurgery*, no. 76, pp. 315–318, 1992.

[10] D. A. Benaron and D. K. Stevenson, "Optical time-of-flight and absorbance imaging of biologic media." *Science*, no. 259, pp. 1463–1466, 1993.

[11] J. C. Hebden, S. R. Arridge, and D. T. Delpy, "Optical imaging in medicine: Experimental techniques." *Physics in Medicine and Biology*, no. 42, pp. 825–840, 1997.

[12] D. A. Boas, A. M. Dale, and M. Franceschini, "Diffuse optical imaging of brain activation: approaches to optimizing image sensitivity, resolution, and accuracy." *Neuroimage*, no. 23, pp. S275–S288, 2004.

[13] D. T. Delpy, M. Cope, P. Zee, S. R. Arridge, S. Wray, and J. Wyatt, "Estimation of optical path-length through tissue from direct time of flight measurement." *Physics in medicine and biology*, no. 33, pp. 1433–1442, 1988.

[14] S. Matcher and C. E. Cooper, "Absolute quantification of deoxyhaemoglobin concentration in tissue near infrared spectroscopy." *Physics in medicine and biology*.

[15] G. Strangman, D. A. Boas, and J. P. Sutton, "Non-invasive neuroimaging using near-infrared light." *Biological Psychiatry*, no. 52, pp. 679–693, 2002.

[16] U. Chaudhary, "Functional near infrared spectroscopy study of language, joint attention and motor skills." Ph.D. dissertation, Florida International University, 2013.

[17] F. Plum and J. B. Posner, *The diagnosis of stupor and coma.*, F. Davis, Ed., 1966.

[18] E. Smith and M. Delargy, "Clinical review, locked-in syndrome." *BMJ*, no. 330, pp. 406–409, 2005.

[19] A. Ramos Murguialday, J. Hill, M. Bensh, S. Martens, S. Halder, F. Nijboer, B. Schoelkopf, N. Birbaumer, and A. Gharabeghi, "Transition from the locked in to the completely locked-in state: A physiological analysis." *Clinical Neurophysiology*, no. 122, pp. 925–933, 2011.

[20] A. J. Haig, R. T. Katz, and V. Sahgal, "Mortality and complications of the locked-in syndrome." *Archives of Physical Medicine and Rehabilitation*, no. 68, 1987.

[21] G. Bauer, F. Gerstenbrand, and E. Rumpl, "Varieties of the locked-in syndrome." *J Neurol*, no. 221, p. 77–91, 1979.

[22] A. Zeman, "What is consciousness and what does it mean for the persistent vegetative state?" *Advances in Clinical Neuroscience and Rehabilitation*, vol. 3, no. 3, pp. 12–14, 2003.

[23] O. N. Markand, "Electroencephalogram in "locked-in" syndrome." *Electroencephalography Clinical Neurophysiology*, vol. 40, 1976.

[24] L. P. Rowland and N. Shneider, "Amyotrophic lateral sclerosis." *The New England Journal of Medicine*, p. 13, 2001.

[25] L. C. Wijesekera and P. N. Leigh, "Amyotrophic lateral sclerosis." *Orphanet Journal of Rare Diseases*, vol. 4, no. 1, p. 3, 2009.

[26] M. C. Kiernan, S. Vucic, B. C. Cheah, M. R. Turner, A. Eisen, O. Hardiman, J. R. Burrell, and M. C. Zoing, "Amyotrophic lateral sclerosis." *The Lancet*, vol. 377, no. 9769, pp. 942–955.

[27] W. F. of Neurology Research Group on Neuromuscular Diseases, "El escorial world federation of neurology criteria for the diagnosis of amyotrophic lateral sclerosis." *Journal of the Neurological Sciences*, pp. 96–107, 1994.

[28] B. R. Brooks, R. G. Miller, M. Swash, and T. L. Munsat, "El escorial revisited: revised criteria for the diagnosis of amyotrophic lateral sclerosis." *Amyotroph Lateral Sclerosis Other Motor Neuron Disorders*, vol. 1, pp. 293–299, 2000.

[29] N. Birbaumer, N. Ghanayim, T. Hinterberger, I. Iversen, B. Kotchoubey, and A. Kubler, "A spelling device for the paralysed." *Nature*, no. 398, pp. 297–303, 1999.

[30] Nirx medical technologies, llc. [Online]. Available: https://nirx.net

[31] Brain products gmbh. [Online]. Available: https://www.brainproducts.com

[32] A. Naro, R. S. Calabrò, M. Russo, A. Leo, P. Pollicino, A. Quartarone, and P. Bramanti, "Can transcranial direct current stimulation be useful in differentiating unresponsive wakefulness syndrome from minimally conscious state patients?" *Restorative Neurology and Neuroscience*, no. 33, pp. 159, 176, 2015.

[33] J. M. O'Toole and G. B. Boylan, "Neural: quantitative features for newborn eeg using matlab." *ArXiv e-prints*, 2017.

[34] Q. Chen, M. Zhang, and B. Xue, "Feature selection to improve generalisation of genetic programming for high-dimensional symbolic regression." *IEEE Transactions on Evolutionary Computation*, vol. 21, pp. 792 – 806, 2017.

[35] S. Wang, J. Tang, and H. Liu, *Encyclopedia of Machine Learning and Data Mining*, SpringerScience+BusinessMedia, Ed., 2016.

[36] G. Chandrashekar and F. Sahin, "A survey on feature selection methods." *Computers and Electrical Engineering*, vol. 40, pp. 16–28, 2014.

[37] T. Lan, D. Erdogmus, A. Adami, M. Pavel, and S. Mathan, "Salient eeg channel selection in brain computer interfaces by mutual information maximization." *Proceedings of the 2005 IEEE Engineering in Medicine and Biology 27th Annual Conference*, pp. 7064–7067, 2005.

[38] H. Peng, F. Long, and D. C, "Feature selection based on mutual information: Criteria of max-dependency, max-relevance, and min-redundancy." *IEEE Transcrictions On Pattern Analysis And Machine Intelligence*, vol. 27, no. 8, pp. 1226–1238, 2005.

[39] G. Roffo, S. Melzi, U. Castellani, and A. Vinciarelli, "Infinite latent feature selection: A probabilistic latent graph-based ranking approach." in *2017 IEEE International Conference on Computer Vision (ICCV)*, 2017.

[40] G. Roffo, S. Melzi, and M. Cristani, "Infinite feature selection." in *2015 IEEE International Conference on Computer Vision (ICCV).*, 2015, pp. 4202–4210.

[41] G. R. Müller-Putz, R. Scherer, C. Brunner, R. Leeb, and G. Pfurtscheller, "Better than random? a closer look on bci results." *International Journal of Bioelectromagnetism*, vol. 10, no. 1, pp. 52–55, 2008.

Acknowledgments

The biggest thanks to my supervisors Ujwal Chaudhary and Professor Dr. Niels Birbaumer who gave me the possibility to join their group at the Institute of Medical Psychology and Behavioral Neurobiology of Tübingen, as well as all the guys who worked with me: Alessandro, Andres, Majid, and Aygul. I couldn't have asked for a better internship, I had the opportunity to grow personally and professionally and get inspired by some of the best people in the BCI field.

A special thank goes to the Furin family who welcomed us during a week of acquisitions with unbelievable serenity and kindness.

I am beyond grateful to my parents Tiziana e Giorgio and my brothers, Enrico e Francesco, for always being my first supporters, advisors and inspires.

Thanks to all the people who have been part of my life in the too fast five years of university: the flatmates, the historical ones of via del Portello and the short-yet-intense ones of via Tiepolo, but also the international ones of calle San Bernardino and DoblerStraße; the course mates, in particular Davide who shared with me the first and last day of university; the endless Padua aperitifs mates; the Erasmus mates; the friends still there since high school; who crossed borders to visit me.

Thanks to Angelo il Virtuosissimo, who, in his own quirky way, through the years, always pushed me further.

Finally, thanks to everyone who will celebrate with me today this nice achievement.

Piazzola sul Brenta, 26th September 2018